




## A new otter of giant size, *Siamogale melilutra* sp. nov. (Lutrinae: Mustelidae: Carnivora), from the latest Miocene Shuitangba site in north-eastern Yunnan, south-western China, and a total-evidence phylogeny of lutrines

Xiaoming Wang, Camille Grohé, Denise F. Su, Stuart C. White, Xueping Ji, Jay Kelley, Nina G. Jablonski, Tao Deng, Youshan You & Xin Yang


To cite this article: Xiaoming Wang, Camille Grohé, Denise F. Su, Stuart C. White, Xueping Ji, Jay Kelley, Nina G. Jablonski, Tao Deng, Youshan You & Xin Yang (2017): A new otter of giant size, *Siamogale melilutra* sp. nov. (Lutrinae: Mustelidae: Carnivora), from the latest Miocene Shuitangba site in north-eastern Yunnan, south-western China, and a total-evidence phylogeny of lutrines, *Journal of Systematic Palaeontology*, DOI: [10.1080/14772019.2016.1267666](https://doi.org/10.1080/14772019.2016.1267666)

To link to this article: <http://dx.doi.org/10.1080/14772019.2016.1267666>

 View supplementary material 

 Published online: 22 Jan 2017.

 Submit your article to this journal 

 View related articles 

 View Crossmark data 

## A new otter of giant size, *Siamogale melilutra* sp. nov. (Lutrinae: Mustelidae: Carnivora), from the latest Miocene Shuitangba site in north-eastern Yunnan, south-western China, and a total-evidence phylogeny of lutrines

Xiaoming Wang<sup>a,b,c,\*</sup>, Camille Grohé<sup>a,b</sup>, Denise F. Su<sup>d</sup>, Stuart C. White<sup>e</sup>, Xueping Ji<sup>f,c</sup>, Jay Kelley<sup>g,h</sup>, Nina G. Jablonski<sup>i</sup>, Tao Deng<sup>c</sup>, Youshan You<sup>j</sup> and Xin Yang<sup>k</sup>

<sup>a</sup>Department of Vertebrate Paleontology, Natural History Museum of Los Angeles County, 900 Exposition Blvd., Los Angeles, CA 90007, USA; <sup>b</sup>Division of Paleontology, American Museum of Natural History, Central Park W. at 79<sup>th</sup> St., New York, NY 10024, USA; <sup>c</sup>Key Laboratory of Vertebrate Evolution and Human Origins of Chinese Academy of Sciences, Institute of Vertebrate Paleontology and Paleoanthropology, Chinese Academy of Sciences, Beijing 100044, China; <sup>d</sup>Department of Paleobotany and Paleocology, Cleveland Museum of Natural History, 1 Wade Oval Drive, University Circle, Cleveland, Ohio 44106, USA; <sup>e</sup>School of Dentistry, University of California, Los Angeles, 10833 Le Conte Ave., Los Angeles, California 90095, USA; <sup>f</sup>Yunnan Institute of Cultural Relics and Archaeology, 15-1, Chunmingli, Chunyuan Xiaoqu, Kunming, Yunnan 650118, China; <sup>g</sup>Institute of Human Origins and School of Human Evolution and Social Change, Arizona State University, PO Box 874101, Tempe, Arizona 85287, USA; <sup>h</sup>Department of Paleobiology, National Museum of Natural History, Smithsonian Institution, Washington, DC 20013, USA; <sup>i</sup>Department of Anthropology, Pennsylvania State University, University Park, Pennsylvania 16802, USA; <sup>j</sup>Zhaotong Institute of Cultural Relics, Zhaotong, 657000, Yunnan, China; <sup>k</sup>Zhaoyang Museum, Zhaotong, 657000, Yunnan, China

(Received 18 May 2016; accepted 20 October 2016)

Otters (subfamily Lutrinae) are semi-aquatic predators in the family Mustelidae. Modern otters have a worldwide distribution but their fossil record is poor, often consisting of fragmentary jaws and teeth. Multiple lineages have developed bunodont dentitions with enlargements of molars, usually for cracking molluscs or other hard foods. Some lineages have evolved badger-like teeth and, as a result, were often confused with melines (Old World badger clade). *Siamogale thailandica* Ginsburg, Invagat, & Tassy, 1983 from the middle Miocene basin of Mae Moh in northern Thailand is one such species, whose fragmentary dental remains have thus far impeded our understanding. A new species of fossil otter, *Siamogale melilutra* sp. nov., represented by a nearly complete cranium, mandible and partial skeletons of at least three individuals, was recovered from the latest Miocene (~6.2 Ma) lignite beds of the Shuitangba Site in north-eastern Yunnan Province, south-western China. Computed tomography (CT) restoration of the crushed skull reveals a combination of otter-like and badger-like cranial and dental characteristics. The new species belongs to the Lutrinae because of its possession of a large infraorbital canal and ventral expansion of the mastoid process, among other traits. A distally expanded M1, however, gives a badger-like appearance. In overall morphology the Shuitangba otter is closest to *Siamogale thailandica*. A previously described jaw ('*Lutra*' *aonychooides*) from the early Pliocene of the Yushe Basin in north China is also here referred to *S. melilutra*. No previous attempt has been made to provide a global phylogenetic framework for otters. We present the first combined morphological and molecular (nuclear and mitochondrial DNAs) character matrices of five extant (*Pteronura*, *Lontra*, *Enhydra*, *Aonyx*, *Lutra*) and eight extinct genera (*Tyrrhenolutra*, *Paralutra*, *Paludolutra*, *Enhydritherium*, *Siamogale*, *Vishnuonyx*, *Sivaonyx*, *Enhydriodon*) to better understand the evolution of bunodont otters. Parsimony and Bayesian analyses consistently recover an eastern Asian clade that includes forms from Shuitangba, Yushe and Mae Moh, all of which are referred to *Siamogale*.

<http://zoobank.org/urn:lsid:zoobank.org:pub:5C637018-0772-4C78-AA4B-783B71085D9D>

**Keywords:** Miocene; fossil otter; lutrine; phylogeny; China; Southeast Asia

### Introduction

Well-preserved otter material of giant size, including crania, mandibles and postcranials, was recently unearthed from the latest Miocene lignite beds of Shuitangba in Yunnan Province (Ji *et al.* 2013; Jablonski *et al.* 2014) and represents a new species of fossil otter (Fig. 1). The

new discovery permits recognition of a rare clade of otters and affords an opportunity to explore relationships among several enigmatic fossil mustelids that have been referred either to badgers or to otters. The modern otter subfamily (Lutrinae) and the Old World badger subfamily (Melinae) share a number of cranial and dental similarities, including enlarged upper and lower molars, which have been

\*Corresponding author. Email: [xwang@nhm.org](mailto:xwang@nhm.org)

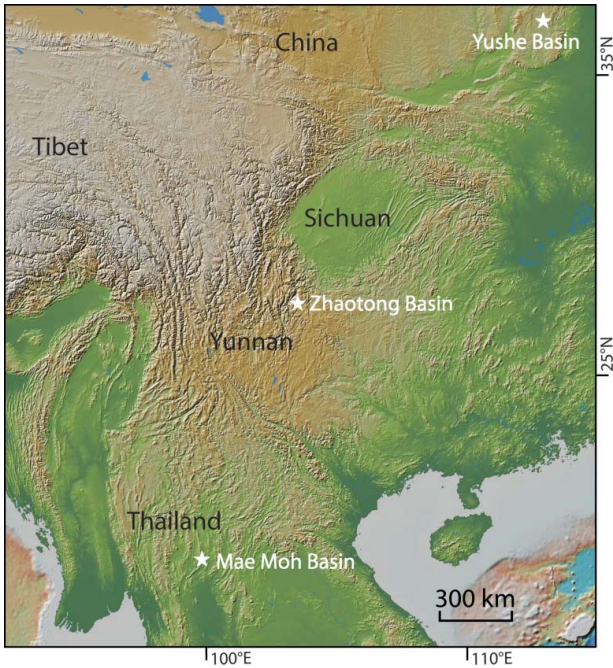


**Figure 1.** Location of Shuitangba (late Miocene) in the Zhaotong Basin, Yunnan Province, the Yushe Basin (Pliocene), Shanxi Province, China, and the Mae Moh Basin (middle Miocene), Lampang Province, Thailand. Topographical map generated by GeoMapApp (version 3.5.1) (Ryan *et al.* 2009).

used as evidence of relationships (e.g. Bryant *et al.* 1993). Such similarities are also found among their fossil representatives, and as increasingly older (and often poorer) specimens are referred to the two subfamilies, a number of mustelid specimens that possess unique combinations of characters have proved challenging to reconcile with existing notions of these subfamilies. These specimens tend to share a peculiar mixture of an enlarged M1 talon, often seen among Old World badgers, and a crested P4 protocone and broadened m1 talonid, characteristic of most living otters. Examples of these puzzling carnivorans include the Miocene genera *Mionictis* from North America, *Lartetictis* from Europe and *Siamogale* from Asia. All of them were initially known only from fragmentary jaws and teeth, and their subfamily identity remains obscure. Such a mixture of badger and otter dental features understandably led to the postulation that lutrines originated from melines, beginning in a transitional form of *Mionictis* (Willemsen 1992).

This paper presents a detailed study of the new fossil otter species from Shuitangba. We describe a new clade of otters and explore relationships of a number of genera of previously uncertain relationships. Unexpectedly, a previously described mandible from the early Pliocene of Yushe Basin in the Chinese Loess Plateau can also be referred to the same species as the otter from Yunnan. Such a linkage has interesting implications for zoogeography and interpreting the habitats to which the newly described otter species was adapted.

## Institutional abbreviations

**AMNH(M):** Collection of the Department of Mammalogy, American Museum of Natural History, New York, USA; **F:AM:** Frick Collection, American Museum of Natural History, New York, USA; **FM:** Fossil Mammals, American Museum of Natural History, New York, USA; **FMNH:** Field Museum of Natural History, Chicago, Illinois, USA; **IVPP:** Institute of Vertebrate Paleontology and Paleoanthropology, Beijing, China; **LACM:** Natural History Museum of Los Angeles County, Los Angeles, USA; **PMU:** Palaeontology collections, Museum of Evolution, Uppsala University, Uppsala, Sweden; **THP:** Tianjin Hoangho-Paiho Museum, Tianjin, China; **ZT:** Zhaotong collection, Yunnan Institute of Cultural Relics and Archaeology, Kunming, Yunnan Province, China.

## Material and methods

The following taxa of extant mustelids have been examined in this study: *Martes americana* (AMNH(M) 165630, Canada; LACM 92400, Alaska); *Galictis cuja* (AMNH(M) 32281, Chile); *Aonyx* sp. (LACM 43468, unknown locality); *Aonyx capensis* (AMNH(M) 55230, Kenya); *Enhydra lutris* (LACM 28155, Alaska; LACM 54425, California; AMNH(M) 24186, Alaska), *Lutra lutra* (FMNH 84806, India), *Lontra canadensis* (LACM 30138, Idaho; AMNH(M) 254475, Florida), *Lontra felina* (FMNH 24225, Chile), and *Pteronura brasiliensis* (FMNH 98077, Peru; AMNH(M) 71858, Peru).

Digital data of the holotype cranium (ZT-10-03-064b) and a right mandibular corpus and ramus (IVPP V 23271) were acquired separately by X-ray micro computed tomography ( $\mu$ CT) using equipment developed by the Institute of High Energy Physics, Chinese Academy of Sciences (CAS), housed in the Key Laboratory of Vertebrate Evolution and Human Origins (Beijing), operating at a flux of 450 kV and 1.5 mA. Raw 16-bit images were obtained at a resolution of 160  $\mu$ m per voxel using a 360° rotation with a step size of 0.25° and an unfiltered aluminium reflection target. These raw images in a 2048  $\times$  2048 matrix of 2048 slices were converted to TIFF images using Adobe Photoshop and imported into Fiji (V. 2.0.0) (Schindelin *et al.* 2012) where they were cropped to the size of the specimens, contrast adjusted and converted to 8-bit TIFF files. The resulting TIFF images were imported into Avizo 9.0.1 Lite (FEI Visualization Sciences Group) for analysis. In Avizo the digitized cranium was segmented into 201 individual fragments, and each was made into a virtual volume. These virtual fragments were then individually transformed (oriented in three-dimensional space) to align them with respect to their neighbours to form a reconstruction of the cranium. The hemi-mandible was represented by a single volume and combined with the cranium model without a change of scale.

We used Mesquite (Maddison & Maddison 2015) to generate the morphological matrix of characters (37 craniodental characters) for 11 fossil otter taxa (at the generic or species level) and eight extant species: six extant otter species (*Pteronura brasiliensis*, *Lontra canadensis*, *Lontra felina*, *Enhydra lutris*, *Lutra lutra*, *Aonyx capensis*) plus *Martes americana* and *Galictis cuja*. Our coding of fossil bunodont otters depends both on our own observations of the specimens from the Siwaliks and on published sources: Pilgrim (1932), Grohé (2011) for *Vishnuonyx*; Peigné *et al.* (2008), Grohé *et al.* (2013) for *Sivaonyx* (*S. gandakasensis*, *S. bathygnathus*, *S. beyi*); Falconer (1868), Matthew (1929), Geraads *et al.* (2011) for *Enhydriodon* (*E. sivalensis*, *E. falconeri*, *E. dikkikae*). Other fossil taxa included in our cladistic analysis are coded mainly based on illustrations and descriptions from the literature: Roman & Viret (1934), Helbing (1936) for *Paralutra jaegeri*; Willemsen (1983), Villier *et al.* (2011) for *Paralutra garganensis*; Ginsburg *et al.* (1983), Villalta & Crusafont-Pairó (1945), Hürzeler (1987) for *Tyrrhenolutra helbingi*; Morales & Pickford (2005) for *Paludolutra* (*P. lluecai*, *P. marammena*, *P. campanii*); Berta & Morgan (1985), Lambert (1997) for *Enhydritherium terranova*; Zdansky (1924) for '*Lutra aonychooides*'. Finally, coding for extant lutrines and *Siamogale* is mostly based on our own examination of specimens and from Grohé *et al.* (2010) and Grohé (2011). We did not include the African bunodont genus *Djourabus* (Peigné *et al.* 2008), which is too poorly known to code.

Our choice of outgroups is based on molecular phylogenies of extant mustelids (such as Koepfli *et al.* 2008a; Sato *et al.* 2012), which suggest that *Martes* is likely to possess the most basal morphological characteristics from which the mustelines and ictonychines have evolved. Furthermore, the ictonychines are either sister to or close to the base of the lutrines and thus we used *Galictis* as a second outgroup. In this context, we did not use *Potamotherium* as an outgroup, as it has been postulated to be an ancestral lutrine by several early studies (Thenius 1949b; Savage 1957; Fahlbusch 1967; Sokolov 1973; Willemsen 1992) but not by others (Muizon 1982). Whether *Potamotherium* is a musteloid or related to the origin of the pinnipeds (Rybczynski *et al.* 2009), its phylogenetic position is considered too doubtful to include in an otter phylogeny.

We downloaded from GenBank the nuclear and mitochondrial gene sequences (21 nuclear partial sequences and one mitochondrial complete sequence) used by Koepfli *et al.* (2008a) in their molecular phylogenetic study of mustelids (list of accession numbers on GenBank available in Koepfli *et al.* 2008a, additional file 6). Only one gene sequence is missing in our data set for *Galictis cuja* (BRCA1 fragment 2 of Koepfli *et al.* 2008a). We aligned each of the nucleotide sequence on SeaView version 3.2 (Galtier *et al.* 1996) running the MUSCLE program, and we exported the aligned sequences as separate Nexus files.

Question marks were used for the missing sequence, insertions and deletions. We concatenated both morphological and molecular data on Mesquite. The supermatrix includes a total of 11,911 characters with 37 craniodental characters and 11,874 base pairs (Supplemental Appendices 1 and 2).

We first ran a parsimony analysis on PAUP\* version 4.0a147 (Swofford 2002) using a heuristic search with random addition sequence, tree bisection-reconnection (TBR) branch swapping, and 1,000 replicates of the random addition sequence. We also ordered one character (27: P4 parastyle). We then created 23 partitions for our data set for Bayesian analysis. The number of partitions was determined after searching for the best-fit models of nucleotide substitution for each gene sequence using the Akaike information criterion (AIC) in MrModeltest version 2.3 (Nylander 2008). We created one partition for morphological data following an Mk model of discrete character evolution (Lewis 2001) and 22 partitions for molecular data following the models presented in Supplemental Appendix 3. We conducted three Bayesian inference analyses on MrBayes version 3.2.6 (Ronquist *et al.* 2012) using this set of partitions, ordering character 27, and running four Markov chains for 10,000,000 generations, sampling trees every 1,000 generations (Supplemental Appendix 4). We assessed stationarity of the chains on Tracer version 1.6 (Rambaut *et al.* 2013); trees generated before stationarity were discarded as 'burn-in' (15% of the trees in our analyses). The three Bayesian analyses gave the same tree topology. After each set of analyses (parsimony and Bayesian), we estimated the robustness of the tree nodes by bootstrap values for the parsimony analysis on PAUP\*, and posterior probabilities for Bayesian analysis on MrBayes.

## Systematic palaeontology

Order **Carnivora** Bowdich, 1821

Infraorder **Arctoidea** Flower, 1869

Parvorder **Mustelida** Tedford, 1976

Family **Mustelidae** Fischer de Waldheim, 1817

Subfamily **Lutrinae** Bonaparte, 1838

*Siamogale* Ginsburg, Ingavat & Tassy, 1983

**Type species.** *Siamogale thailandica* Ginsburg, Ingavat & Tassy, 1983.

**Included species.** *Siamogale thailandica* Ginsburg, Ingavat & Tassy, 1983 and *Siamogale melilutra* sp. nov.

**Emended diagnosis.** *Siamogale* has typical lutrine cranial and dental morphologies: a large infraorbital canal, presence of antorbital fossa, uninflated bulla, robust and protruding mastoid process, mastoid process separated by a broad shelf from the paroccipital process, postglenoid

foramen positioned anteriorly to the auditory meatus, inion positioned anteriorly relative to the lambdoid crest, stylomastoid foramen separated by a bony ridge from the tympanohyal-bulla connection, masseter muscle attachment area ventrally expanded to beyond the ventral rim of the masseteric fossa, parallel zygomatic arches, shortened angular process, premolars with surrounding cingulum, shortening of P4 metastylar blade, presence of a notch between talonid and trigonid of m1, and widening of m1 talonid. *Siamogale* differs from *Paralutra jaegeri* by the presence of a distal ridge of m1 metaconid connected to the entoconid crest, M1 cuspule distal to metacone, and absence of P4 metastylar notch. *Siamogale* differs from *Paludolutra*, *Tyrrhenolutra* and *Enhydritherium* in having a crestiform protocone, lack of hypocone and presence of parastyle on P4, a distolingually expanded M1 talon, and metaconule placed distally to the metacone.

**Remarks.** Among known fossil taxa, the Shuitangba species is closest to *Siamogale thailandica*. They both display a metaconid distal ridge on m1, a cusp-like P4 protocone, and an M1 with a cuspule present just distal to the metacone. Thenius (1949a) was the first to recognize an affinity of the French Miocene ‘*Lutra*’ *dubia* Blainville, 1841 from Sansan with the North American *Mionictis* (Matthew 1924) from the early Barstovian lower Snake Creek beds, a notion followed by Ginsburg (1961, p. 123) in his description of Sansan carnivorans. Later, in his study of Miocene ‘piscivores’ from France, Ginsburg (1968) described a second species of European *Mionictis*, ‘*M.*’ *artenensis*, and erected a new tribe, Mionictini, under the subfamily Melinae. Additional fragmentary materials were referred to *Mionictis* from the early and middle Miocene of France (Ginsburg & Bulot 1982) and the middle Miocene of Saudi Arabia (Thomas *et al.* 1982), and another species, ‘*M.*’ *ginsburgi*, was recovered from the late Miocene of Spain (Alcalá *et al.* 1994). The latter is almost certainly a true meline and was later given separate generic status as *Adroverictis* Ginsburg & Morales, 1996. Moreover, the European ‘*M.*’ *dubia* was also given a separate generic status, *Lartetictis*, under the subfamily Melinae (Ginsburg & Morales 1996, 2000), even though it has also been described as a member of the subfamilies ‘Mustelinae’ (Heizmann & Morlo 1998) and Lutrinae (Ginsburg 1999). Finally, ‘*M.*’ *artenensis* was attributed to the genus *Trochictis* and placed within the Mellivorinae (Ginsburg & Morales 1992) and Melinae (Ginsburg & Morales 1996, 2000). The European mionictines thus increasingly assumed badger identity with successive iterations of studies by Ginsburg and Morales. Grohé *et al.* (2010) made detailed and extensive comparisons between *Siamogale* and European and North American mionictines. Most recently, Salesa *et al.* (2013) described a new genus and species, *Teruelictis riparius*, from the late Miocene of Spain and, together with *Lartetictis dubia*, considered it a non-aquatic ancestor of lutrines. However, the dental

morphology of *Teruelictis* is quite primitive (presence of a P1 and p1, absence of cingula in premolars, P4 with a simple protocone) and the phylogeny of Lutrinae from Salesa *et al.* is supported by only a single derived dental character (a well-developed M1 talon cingulum) plus two postcranial characters. Membership of *Teruelictis* within the otter clade seems doubtful.

In North America, where the genus was originally named, knowledge of *Mionictis* was largely confined to jaw fragments and lower teeth in the half-century subsequent to its being named (Matthew 1924; Cook & Macdonald 1962), until Harrison (1981) referred to it an M1 from the late Clarendonian WaKeeney Local Fauna of Kansas (originally published by Wilson 1968) and a partial skull and mandible from the Clarendonian MacAdams Quarry of Texas (see Baskin 1998 for additional referred specimens in North America). Unfortunately, more than 90 years after the initial description of the type species, *Mionictis incertus*, there is still no upper dentition from the Snake Creek. We agree with Harrison, however, that the MacAdams Quarry materials (F:AM 63296 and 63298) (see Tseng *et al.* 2009, fig. 11 for an illustration of its P4–M1) are referable to *Mionictis*, so the Texas specimens thus add crucial information about the upper teeth of this elusive genus. In light of the upper dentition from Texas, the case for a badger relationship is strengthened by the presence in *Mionictis* of a postprotocrista on M1, an accessory cuspule on the distolingual aspect of the M1 metacone, and a P4 protocone that is unexpanded distally. Nevertheless, the MacAdams Quarry *Mionictis* shares derived characters with *Siamogale*, such as an enlarged infraorbital canal, a distal crest on the m1 metaconid, and an expanded M1 distolingual border, although the last character is also frequently developed in melines such as *Arctomeles* (Stach 1951; Wallace & Wang 2004), *Melodon* (Zdansky 1924; Tedford & Harington 2003) and *Arctonyx* (Colbert & Hooijer 1953). Consequently, it seems clear that, whether *Mionictis* is a lutrine or a meline, some of the above characters must have evolved independently.

Recent molecular phylogenies of mustelids consistently place the melines and lutrines on the opposite ends of the mustelid clade (e.g. Koepfli & Wayne 1998; J. J. Flynn *et al.* 2005; Koepfli *et al.* 2008a, b; Sato *et al.* 2012), which strongly suggests that morphological characters formerly considered synapomorphies between badgers and otters (Bryant *et al.* 1993) are likely the result of convergences. Sorting out these convergences, however, is fraught with hazards, especially for taxa that have no modern descendants. Within the framework of molecular phylogenies, such as that by Sato *et al.* (2012), the basal position of melines within living mustelids suggests that the presence of a postprotocrista on M1 in the badgers is a primitive condition, as seen in all non-mustelid carnivorans, and its absence is a derived condition starting somewhere near *Martes* and persisting through lutrines – that

is, loss of the postprotocrista is not homoplastic. As for the accessory cusp behind the M1 metacone, it is largely confined to the meline clade (Wallace & Wang 2004), although this cusplule is also seen in *Melogale* (Teilhard de Chardin & Leroy 1945; Storz & Wozencraft 1999). With the molecular constraint, therefore, upper molars in mionictines (*Mionictis*, *Lartetictis*, *Adroverictis*, *Trochictis*) present a meline plan, as Ginsburg & Morales (1996) had envisioned. Our exclusion of mionictines from lutrines, however, implies that the post-metacoid ridge on the m1s of *Siamogale* was acquired independently from that in mionictines.

Most recently, Smith *et al.* (2014) described a new genus and species, *Negodiaetictis rugatrulleum*, from the middle Miocene (Barstovian) Monarch Mill Formation of west-central Nevada. The Nevada form, limited to a partial dentary with p3–m1 and an isolated m2, shows some resemblance to *Siamogale* in its crowded premolars, highly wrinkled enamel surface in both premolars and molars, surrounding cingulum in the premolars, an incipient development (relative to *Siamogale*) of a distal ridge

on the m1 metaconid that connects with the entoconid crest, and a basined m1 talonid. Although Smith *et al.* refrained from including *Negodiaetictis* in a particular mustelid clade, they allowed that *Mionictis* may be the most comparable to their new genus. It is conceivable that it may be related to *Siamogale*, but *Negodiaetictis* is too poorly known to be certain if it is a lutrine or a meline.

*Siamogale melilutra* sp. nov.  
(Figs 2–11, 13)

1945 *Lutra aonychoides* Zdansky; Teilhard de Chardin & Leroy: 21, fig. 12.

2014 *Siamogale* sp. nov. Jablonski, Su, Flynn, Ji, Deng, Kelley, Zhang, Yin, You, & Yang: table 1, fig. 3D.

**Diagnosis.** *Siamogale melilutra* is distinct from *S. thailandica* in its large size, more posteriorly reclined mandibular ascending ramus, a continuous P4 protocone crest extending distally to the metastyle (in contrast to a more cuspidate P4 protocone in *S. thailandica*), a relatively less distally expanded M1 lingual cingulum, a more shortened

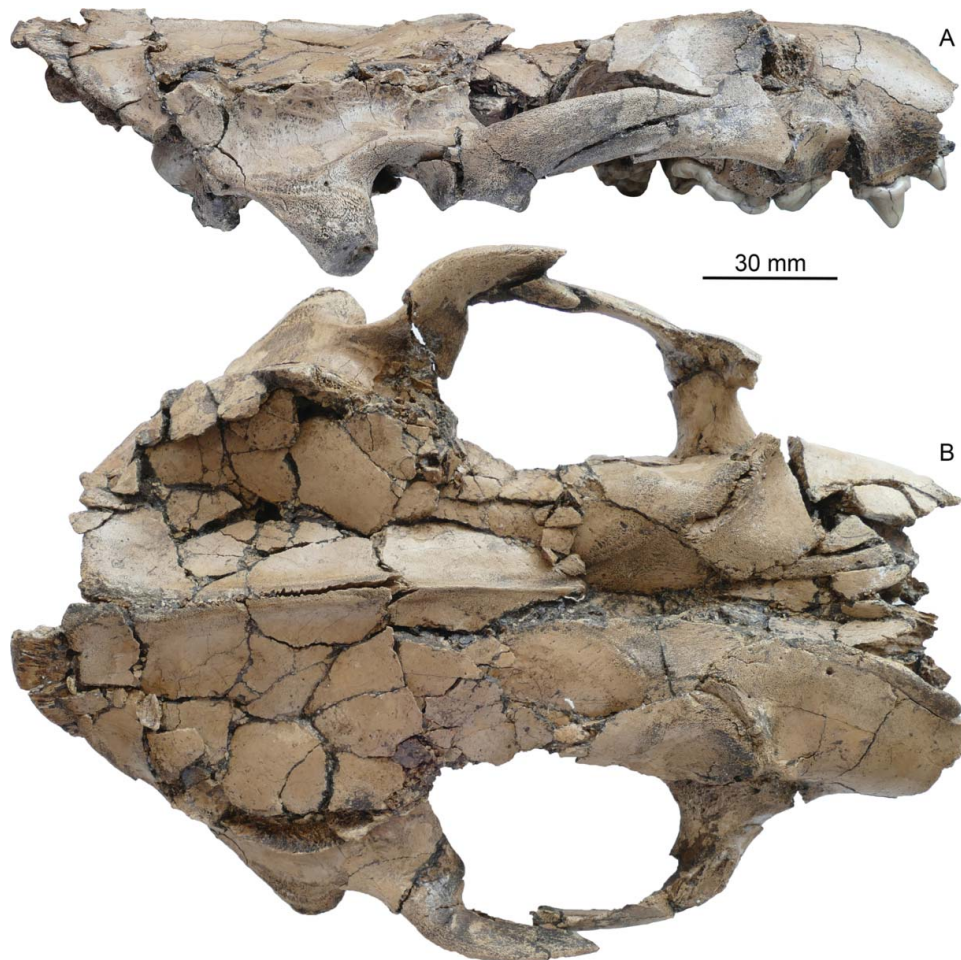


**Figure 2.** Cranium of *Siamogale melilutra* sp. nov., ZT-10-03-064b, holotype from Shuitangba. **A**, right lateral, and **B**, dorsal views.



**Figure 3.** Cranium of *Siamogale melilutra* sp. nov., ZT-10-03-064b, holotype from Shuitangba. **A**, left lateral, and **B**, ventral views.

m1, and an m1 metaconid ridge being differentiated into a discrete metastylid.

**Etymology.** *mēlēs* and *melis* (feminine), Latin, badger; *lutra* (feminine), Latin, otter; a reference to the mixture of typically lutrine and meline cranial and dental morphology in this species.

**Holotype.** ZT-10-03-064b, partial cranium with left P3–M1 and right P2–M1 (Figs 2–5, 8).

**Referred specimens.** ZT-09-03-032, basicranium and other skull fragments with isolated left I1–3, P2–3, and M1, and right I1–3 and P2 (broken)–M1, from first lignite bed (Fig. 9); IVPP V 23269 (ZT-15-0002), right basicranial region, from upper part of layer 7 (peat) (Fig. 5B); IVPP V 23270 (ZT-15-0387), partial, pathological left dentary with c alveolus, p4, and m1–2 alveolus, from upper part of layer 10 (Figs 6, 10A); IVPP V 23271 (ZT-15-0968), nearly complete right dentary (missing dorsal tip of ascending ramus) with i1–3 alveoli, c, p2–3 alveoli, p4–m1, and m2 alveolus, from upper part of layer 11 (T6)

(Fig. 7, 10B); IVPP V 23272 (ZT-15-01497), isolated right M1, from upper part of layer 11 (T7); ZT-07-02-274, isolated right m2 (Fig. 10C); ZT-10-0375, distal left humerus, from bottom of layer 10 (maximum distal condyle width 47 mm); ZT-10-0077, complete right femur, from bottom of layer 9 (maximum length 162 mm; maximum distal condyle width 40 mm); ZT-10-01-0013, complete right tibia (maximum length 143 mm; maximum proximal condyle width 40 mm); ZT-10-0008, left astragalus, from layer 6; ZT-09-03-423, left astragalus, from layer 9 (maximum proximodistal length 28.06 mm; maximum mediolateral width 30.50).

From Yushe Basin, THP 19898 (FM cast 143941), nearly complete left dentary with i3–c alveoli, p2–m1, and m2 alveolus (Fig. 11); this specimen was collected from Dapinggou by E. Licent, probably in the Taoyang Member of Gaozhuang Formation, ~4.9–5.4 Ma (Opdyke *et al.* 2013).

**Type locality.** The Shuitangba (‘Water Pond Platform’ in Chinese) fossil site is within an open-pit lignite mine near

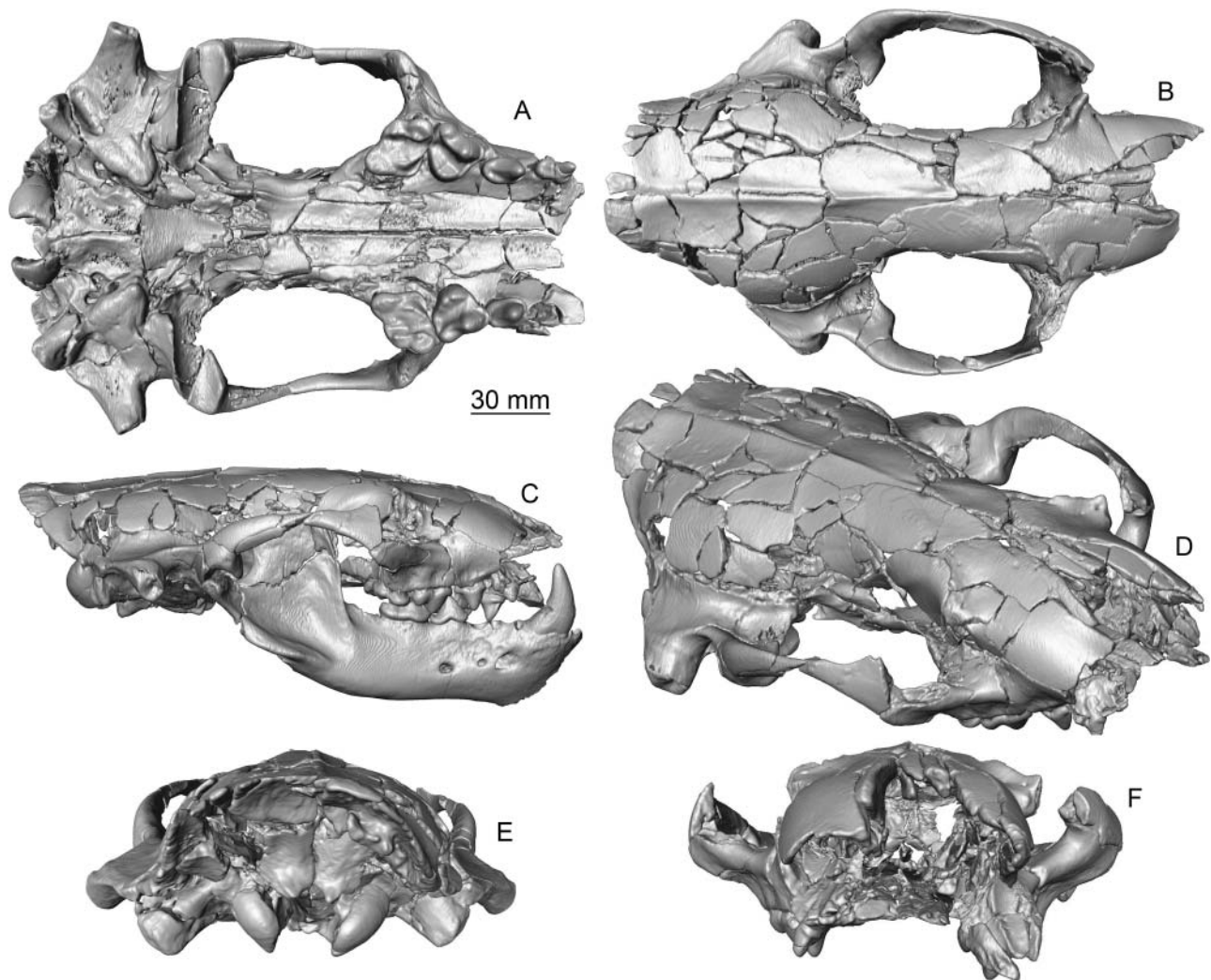


**Figure 4.** Digitally restored cranium of *Siamogale melilutra* sp. nov., ZT-10-03-064b, holotype from Shuitangba, plus a right mandible, IVPP V 23271 (in C only). A, ventral, B, dorsal, C, right lateral, D, anterior oblique, E, posterior and F, anterior views.

the city of Zhaotong, at the margin of a sub-basin within the Zhaotong Basin, in north-eastern Yunnan Province (Jablonski *et al.* 2014) (Fig. 1). Fossils were recovered from the Neogene Zhaotong Formation, which consists of three lignite beds (two of the beds occurring at Shuitangba) of a few metres to tens of metres in thickness (Dai & Chou 2007). Vertebrate fossils have been recovered from dark clays between layers of lignites in the 16 metre section of Shuitangba (Jablonski *et al.* 2014; Zhang *et al.* 2016).

**Associated fauna, flora, age and environment.** Reports by the Yunnan Provincial Museum of the initial discovery in 1960 of a ‘late Pliocene to Pleistocene’ mammal assemblage in the Zhaotong Basin included *Felis* sp., *Zygodon* sp., *Stegodon zhaotongensis*, *Elephas* sp., *Tapirus* sp., *Equus* cf. *yunnanensis*, *Sus* sp., *Muntiacus* and bovids (Chow & Zhai 1962). The precise locality was not known

at the time of these early reports, although the authors compared the fossil matrix with lignite strata in the south-western region of Zhaotong. During the summer of 1978, Shi *et al.* (1981) were able to secure some fossils from a local lignite mine operated by Yongle Village in Dongjin Commune, east of the town of Zhaotong, as well as from Pleistocene gravel beds near Dazhai, in the western part of the basin. From the Yongle lignite bed they described *Sinocastor zhaotongensis*, *Tapirus yunnanensis*, *Metacervulus* sp., *Stegodon* sp. and *Zygodon* sp. The Yongle lignite mine in the 1970s and 1980s is now called Shuitangba, although the mining pit has been moved about a hundred metres to the west since the first discovery of the vertebrate fossils.

The fauna from Shuitangba appears to be of the late Baodean Chinese Land Mammal Age (late Miocene) with typical large mammals such as the deer *Muntiacus* (Dong *et al.* 2014), the tapir *Tapirus* (Ji *et al.* 2015), the



**Table 1.** Cranial measurements (in mm) for *Siamogale melilutra* sp. nov. Measurements for the originally crushed cranium (uncorrected originals) and corresponding measurements on the digital model (by Avizo) after restoration (Fig. 4) are both presented to give a sense of distortions due to flattening of the cranium by sedimentary compaction. The extensive dorsoventral crushing suffered by the cranium (Figs 2, 3) resulted in exaggerations of all width measurements, whereas the length measurements are relatively unchanged.

Measurements	ZT-10-03-064b	
	Uncorrected original	Digitally restored
Distance from inion to anterior-most tip of right maxillary	205	196
Maximum width across zygomatic arches	147	127
Minimum width across medial wall of infraorbital foramen	69	51
Anteroposterior length of temporal fossa (left)	52	59
Maximum width across mastoid processes	145	131
P2–M1 length	60	58
Width across left and right M1s at labial borders	71	67
Minimum width between tympanic bulla	33	22
Distance between lateral tips of occipital condyles	51	39
Width of foramen magnum	18	15
Distance between posterior edge of glenoid fossa and posterior tip of paroccipital process (right side)	44	45
Height between inion and top edge of foramen magnum	44	34

proboscideans *Stegodon* and *Sinomastodon* (Wang *et al.* 2015), and small mammals such as the rodents *Sinocastor*, *Kowalskia* and *Pliopetaurista* (Ji *et al.* 2013; Jablonski *et al.* 2014). Palaeomagnetic studies reveal a normal polarity for the 14 m long Shuitangba fossil section, which, along with a longer drill core (120 m) several hundred metres away, was correlated to the top of subchron C3An.1n through the base of C3An.2n (Ji *et al.* 2013), with an age estimate of 6.03–6.73 Ma (Hilgen *et al.* 2012). However, the beds that produced the otter remains are essentially the same as those from which the hominoid fossils were recovered, which is close to ~6.2 Ma (Ji *et al.* 2013; Jablonski *et al.* 2014).

A new species of fox nut, *Euryale yunnanensis*, was recently described from the Shuitangba site (Huang *et al.* 2015). This aquatic plant is consistent with a shallow lake or swamp environment in a mildly warm and humid climate, also confirmed by sedimentological studies (Zhang *et al.* 2016). Pollen studies suggest a flora associated with the vertebrate fossils of evergreen broad-leaved forests with evergreen *Quercus* as the most dominant element, with expansion of grasses (including Poaceae) and decline of conifers at the otter (and hominoid)-producing horizon (Chang *et al.* 2015).

**Description.** ZT-10-03-064b is a nearly complete cranium of a young adult with most of the sutures unfused and the teeth unworn. Although most of the bones are well preserved, the skull is heavily crushed dorsoventrally resulting in a flattened profile view (Figs 2A, 3A). Because of the immature status of this individual, many

sutures became dislocated from the crushing. The other cranial remains, ZT-09-03-032, on the other hand, show slightly better fusion, making additional observations possible, especially on the basicranial area.

We carried out a complete digital restoration of ZT-10-03-064b based on a high-resolution computed tomography (CT) scan. Despite the heavy dorsoventral crushing, the integrity of most individual bone fragments is relatively good. By segmenting 201 relatively large pieces (virtual volumes) and manually re-aligning the individual pieces to minimize gaps between fragments and to maximize bilateral symmetry, our restoration resulted in a substantially more realistic cranium with minimal distortions (Fig. 4). As shown in Table 1, nearly all measurements in the restored cranium are shorter (and presumably more accurate) than in the heavily distorted original state.

**Cranium (Table 1; Figs 2–5).** Both nasals are incomplete, especially near their anterior ends; the broken surfaces end near the anterior margin of the P3. Their posterior ends are also not clearly visible due to damage in this area, and it is not clear if the nasals are shortened as in some living lutrines. The maximum width of the right nasal is 6.9 mm (on the un-restored original specimen; see Table 1). The premaxilla is broken anteriorly and its anterior portion beyond the maxillary contact is lost. The remaining portion of the premaxilla is a slender process between the nasals and maxilla. The posterior process of the premaxilla extends posterior to the anterior rim of the orbit. The maximum width of the right premaxilla is 5 mm near its anterior end, and the total length is about

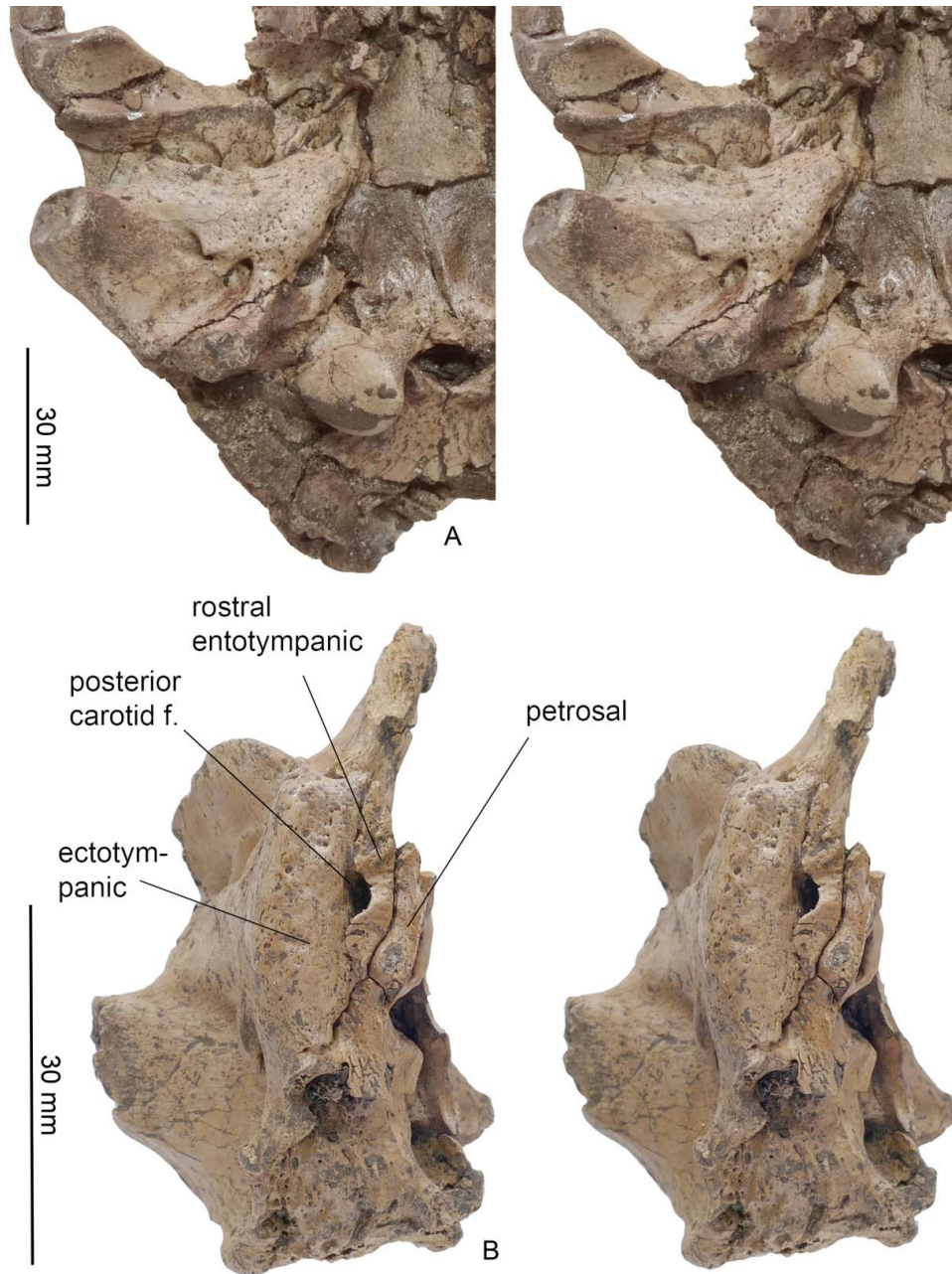


**Figure 5.** Stereo photographs of the right basicranial region of *Siamogale melilutra* sp. nov. **A**, ZT-10-03-064b (ventral view), holotype from Shuitangba. **B**, IVPP V 23269 (naturally dissected; medial view), a referred specimen from Shuitangba.

42 mm. The maxilla is well preserved, especially on the right side. The maxillary-frontal suture is clearly delineated in dorsal view and disjointed to different degrees along its length. The maxillary-jugal sutures are dislocated on both sides and were restored digitally. Both zygomatic arches are largely intact and appear distinctly straight in dorsal view as is seen in some lutrines, in contrast to the laterally arched condition in primitive mustelids. The zygomatic arch is relatively slender with a maximum depth of 12.7 mm near the posterior end. The dorsal roof of the infraorbital canal is broken on both

sides. The dorsal root of the anterior end of zygomatic arch, making up the dorsal roof of the infraorbital canal, is located approximately at the same level as the ventral root, in contrast to the more anteriorly located dorsal root in living lutrines (Holmes 1988), and this is the case after digital restoration as well. The maximum mediolateral diameter of the infraorbital canal is 13.7 mm and the dorsoventral diameter can only be estimated to be around 11 mm, making the cross section of the canal approximately oval shaped. This canal is decidedly enlarged, as is the case in all lutrines. The temporal crests are indistinct

and unite near the anteroposterior midrange of the orbit, about 40 mm posterior to the anterior rim of the orbit. The sagittal crest is a single, low crest, projecting no more than 1 or 2 mm from the cranial surface, probably mostly due to the immature status of this individual. Crushing of the cranium does not permit definitive recognition of a postorbital constriction, although the digital restoration shows slight narrowing, suggesting that there was minimal postorbital constriction. Nor is there clear development of a postorbital process of the frontal (zygomatic process). This minimal constriction stands in contrast to the condition in living lutrines. Nor was the constriction anteriorly shifted as in the latter. The frontal-parietal sutures are mostly disjointed and are generally at a level just posterior to the anterior margin of the glenoid fossa. The lambdoidal crest greatly overhangs the occipital condyles. The inion is slightly anteriorly positioned compared to the lambdoidal crest, as in all living lutrines.

In lateral view, the anterior rim of the infraorbital canal is slightly anterior to the anterior border of the M1. The canal is short, although it is not possible to measure the exact length because of the missing dorsal roof. The postorbital process of the jugal (frontal process) is high, but its dorsal tip is broken.

Ventrally, the entire premaxillary part of the rostrum is missing. The palate is fragmented into several pieces and caved in over large areas, and the anterior margin of the maxilla is not preserved. The maxillary-palatine suture is near the posterior margin of the P4s. The palatine foramen is not clearly discernable. The palatine greatly expands posteriorly, although not reaching the level of the glenoid fossa as in *Arctonyx*. The posterior border of the palatine is approximately 30 mm posterior to the posterior border of the M1s.

Although the basioccipital-basisphenoid region is dislocated from the bullae on either side, the basicranial region is well preserved due to the robust construction of the bullae (Fig. 5A). The basioccipital is broad, as is typical in most arctoids, with the medial borders of the bullae diverging posteriorly. The tympanic bulla is flask-shaped and its anterior end is blunt with a slightly enlarged front tip for the Eustachian canal. It has a rather flat ventral surface, its medial aspect being slightly more inflated, and numerous small pits are present on the surface. The entrance of the carotid artery is located about midway along the medial border of the bulla and posterior to the basisphenoid-basioccipital suture, approaching the condition observed in modern *Lutra* and *Enhydra*, while *Pteronura* and *Aonyx* have a more anteriorly located posterior carotid foramen, at the level of or anterior to this suture (Bryant *et al.* 1993, character 8). The posterior lacerate foramen is separate from the posterior carotid foramen and located posterior to the latter. The jugular and posterior lacerate foramina are confluent, unlike in some modern mustelids, such as *Galictis*, *Lyncodon*, *Mellivora*,

*Taxidea*, *Meles* and *Arctonyx* (Bryant *et al.* 1993, character 10), although there is some polymorphism for this character. The rostral entotympanic runs for a considerable length of the medial face of the ectotympanic but stops at the posterior lacerate foramen. The entire bullar complex is highly specialized with a very long external auditory meatus that is solidly fused with the mastoid process. The postglenoid foramen is flanked posteriorly by the external auditory meatus, as in all living otters. There is no alisphenoid canal. The stylomastoid foramen is separated from the tympanohyal articulation by a bony ridge, as in all living lutrines. The mastoid process is greatly expanded laterally and ventrally, even extending beyond the level of the auditory meatus ventrally, as in living otters. This process has an oval cross section, terminating laterally with a rounded lateral facet that caps the process. The paroccipital process is greatly thickened in ZT-10-03-0064b, but less so in ZT-09-03-032, with a robust, pointed ventral component that has rough surface textures. The base of the paroccipital process is nearly as long as the bulla. The paroccipital process has a flattened cross section in ZT-09-03-032 and is oriented posteriorly. Between the paroccipital and mastoid processes there is a broad shelf posterior to the bulla, typical of all living lutrines.

The isolated right basicranium of IVPP V 23269 (Fig. 5B) offers an opportunity to directly observe the medial and dorsal structures of the petrosal and braincase. In medial view there is a separate bony element medial to and flanking the posterior carotid foramen. This element is probably the rostral entotympanic as questionably identified by Hunt (1974, pl. 8, fig. 27) in *Pteronura*.

**Mandible (Table 2; Figs 6, 7).** A nearly complete right dentary (IVPP V 23271) and a partial left dentary (IVPP V 23270) offer a nearly complete, undistorted view of the mandible. However, IVPP V 23270 is pathological with a swollen corpus at the m1 region, possibly due to infections and subsequent healing when the m1 was lost and its alveoli filled with cancellous bone.

The corpus is robust, particularly in the pathological left corpus. It is nearly straight in the cheek tooth region except for a small process at the base of the symphyseal joint on IVPP V 23270. The anterior part of the mandible in IVPP V 23271 deepens dorsoventrally. On this specimen, the mandibular symphysis extends ventrally between the level of the canine and the anterior alveolus of p2. Posterior to m1, the lower border of the corpus gradually rises and merges with the lower border of the masseteric fossa. As a result, an angular process is noticeably absent, and only hinted at by a small spur at the posterior end. There are two (IVPP V 23270) or three (IVPP V 23271) mental foramina. Those on IVPP V 23270 are anterior to p4 and at the posterior root of p4 (smaller one). The posterior two foramina on IVPP V 23271 are in similar positions to

**Table 2.** Mandibular measurements (in mm) for *Siamogale melilutra* sp. nov. The pathological condition of IVPP V 23270 resulted in considerable thickening of the corpus as well as other modifications, and its measurements should not be considered as being within a normal range of variation.

Measurements	IVPP V 23271	IVPP V 23270
Maximum anteroposterior distance from anterior tip of incisor alveolar border to posterior tip of condyle	145.74	113.04
Maximum anteroposterior distance from anterior tip of incisor alveolar border to posterior edge of ascending ramus above the mandibular condyle (coronoid level)	126.29	109.10*
Anteroposterior distance at base of ascending ramus	35.18	35.33
Height of ascending ramus from lower border of horizontal ramus to top of ascending ramus		58.32
Maximum width of mandibular condyle	37.47	
Maximum depth of horizontal ramus at m1 trigonid	28.66	29.93
Maximum width of horizontal ramus at m1 trigonid	12.86	15.54
Alveolar distance from p2 to m2	62.19	
Alveolar distance from p4 to m2	41.55	43.79

\*coronoid process partially broken.

those in IVPP V 23270, but the posterior-most one is larger and an additional foramen is present at the junction of p2 and p3.

The ascending ramus is moderately tall, measuring 56 mm from the tip of the coronoid process to the ventral border of the masseteric fossa. The anterior border is inclined posteriorly, in contrast to a more erect orientation in living lutrines. The masseteric fossa is deeply excavated, especially at its ventral border. A prominent and sharp lateral ridge forms the ventral rim of the fossa, which protrudes laterally to form a wide ventral shelf. This ventral shelf is distinctly marked by a long scar for the superficial masseter that runs the entire length of the ventral border.

The angular region of the mandible is highly specialized, notably by the near absence of the angular process. In medial view, a small medial-ventral crest marks the location of the pterygoid muscle attachment, possibly a homologous position for the angular process. This remnant of an angular process is not only highly reduced but also very elevated in its position with respect to the mandibular condyle. Anterior to the reduced angular process, on the ventral side of the horizontal ramus, is a shallow but broad scar of unknown derivation, its anterior extent reaching to the m1–2 junction or beyond (in IVPP V 23270).

The mandibular condyle is mediolaterally wide, measuring about 37 mm on IVPP V 23271 and matching the correspondingly wide glenoid fossa on the cranium. Such a wide mandibular joint, coupled with a prominent anterior spur of the glenoid fossa, limits rotation to opening and closing of the jaws and precluding lateral or anteroposterior movements. However, this tight articulation is not interlocking (jaws are easily detached from cranium), unlike the condition in living sea otters.

**Upper teeth (Table 3; Figs 8, 9).** Upper teeth from both ZT-10-03-064b and ZT-09-03-032 are well preserved. Both represent young adults and show practically no wear except on the incisal edges and the cusp tips of the premolars. An isolated right M1 (IVPP V 23272) has modest wear, providing some sense of occlusal wear.

A complete set of upper incisors is preserved on ZT-09-03-032 (Fig. 9). I1s are the smallest. A single main cusp forms the crown with a lingual cingulum forming a distinct V-shape. This cingulum flanks the main cusp and gives a spatulate appearance to the tooth. The I2s are larger than the I1s and similar in shape. The I2 lingual cingulum also forms a strong V shape, although it is not symmetrical, with the mesial side being longer, thicker and taller. The I3s are nearly twice as wide as the I1s. A single main cusp is flanked on the lingual side by a distinct cingulum that thickens towards the base to form a small lingual shelf. The cingulum extends around the labial side and is more wrinkled here than lingually. There is a sharp crest at the distolateral aspect of the I3, extending from the main cusp to the base of the crown. Only a partial alveolus of the right upper canine is preserved on the type specimen, and the preserved part shows a diameter of 16.1 mm in maximum dimension and 10.1 mm in minimum dimension.

There is apparently no P1, although damage to this part of the cranium prevents a definitive assessment; nor can we be sure if this is due to an evolutionary loss or to an individual variation, although we are inclined to the former because of the absence of p1 (see below). The P2 has a single cusp, typical of many arctoid carnivorans. Prominent mesial and distal ridges flank the cusp, and a distinct cingulum surrounds much of the tooth but weakens on the buccal face. This cingulum is particularly strong at the distolingual aspect of the tooth. The P3 is much like the

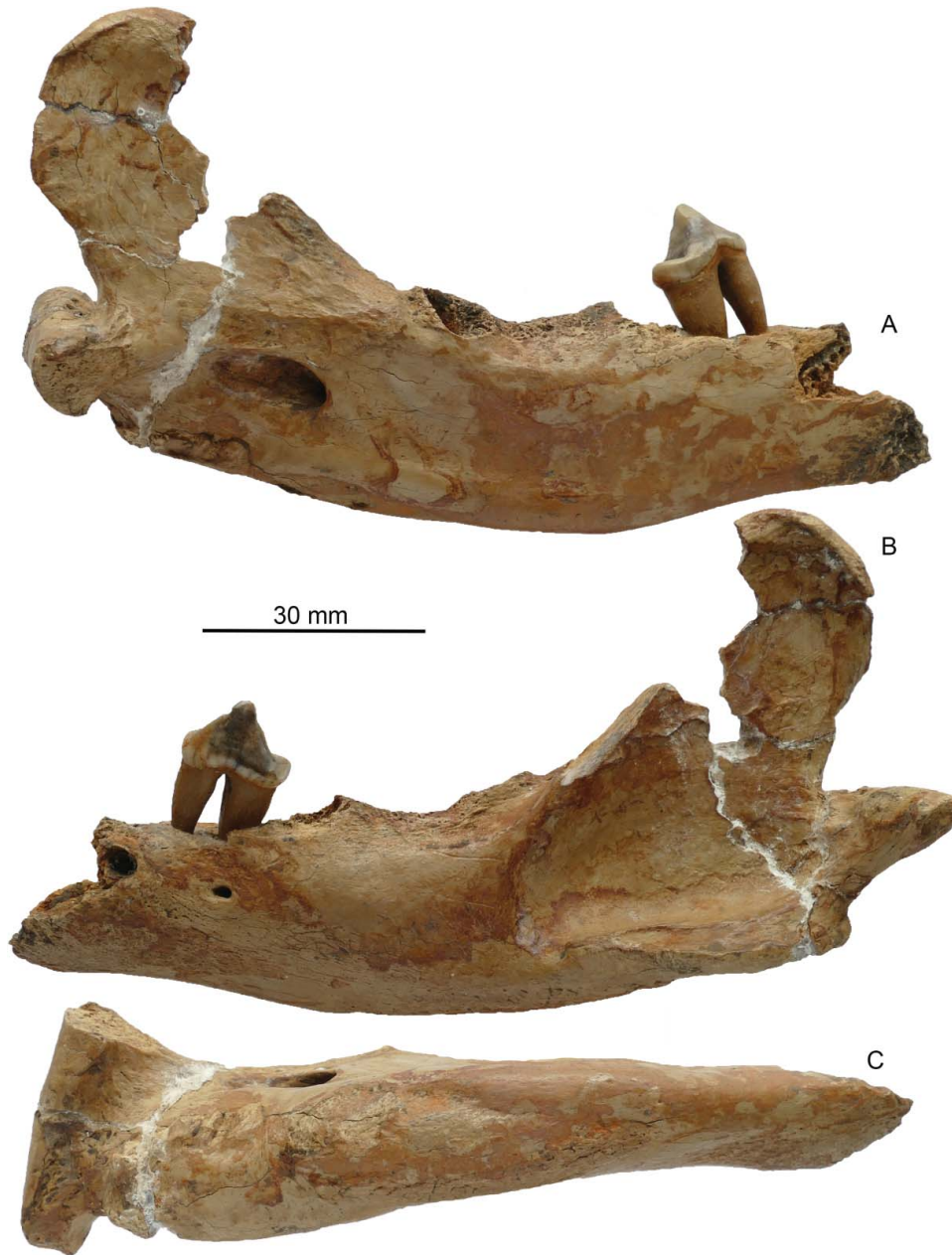


**Figure 6.** Left mandible of *Siamogale melilutra* sp. nov., IVPP V 23270, a referred specimen from Shuitangba. **A**, medial, **B**, lateral, and **C**, ventral views.

P2 except for a prominent swelling on the lingual side. Mesially and distally the cingulum also swells slightly to be almost cusp-like, this being more so in ZT-09-03-032.

The P4 is a large tooth with equal length and breadth and an approximately triangular occlusal outline. The paracone is the tallest cusp. A faint mesial crest arises near the apex of this cusp and ends at its base. The carnassial blade extends distally from the paracone and is not indented by a carnassial notch. Instead, the carnassial blade forms a crest running to the metastyle. A prominent

mesial cingulum surrounds the entire mesial aspect of the tooth. There is a slight thickening at the mesiobuccal corner of the cingulum participating in the formation of a parastyle. The mesial cingulum fades distally and disappears towards the distal base of paracone. The mesiobuccal surface of the metastyle is essentially free of a cingulum. The P4 is perhaps the most lutrine-like tooth with a prominent protocone crest that connects mesially with the mesial cingulum. However, the mesial cingulum continues lingually around the mesiolingual aspect of the protocone crest but



**Figure 7.** Right mandible of *Siamogale melilutra* sp. nov., IVPP V 23271, a referred specimen from Shuitangba. **A**, medial, **B**, lateral, and **C**, ventral views.

the cingulum here is far less distinct than mesially. The protocone crest has a thick base that forms almost the entire lingual half of the tooth, having a highly robust appearance when compared to the thin crest and low shelf in most living lutrines. As a result, the protocone crest is also much higher crowned than its modern counterparts. The protocone crest extends distally to the very end of the metastyle, thus creating a long and deep valley between the crest and the carnassial blade. Much of the protocone crest is free of a cingulum, and in the case of ZT-10-03-064b, a shallow apical notch is present in the middle of the crest, giving the appearance of a separate ‘protocone’ and ‘hypocone’. This notch is largely absent in ZT-09-03-032, even though some crenulations are visible along the distal border of the protocone crest.

The M1 is the largest tooth with greater buccolingual width than mesiodistal length. All cusps are relatively low crowned compared to those of the P4. The paracone and metacone are approximately equal in height and size. However, the paracone is surrounded by a bulging parastyle and buccal cingulum that dwarf the paracone in height, and has an enlarged base at the expense of the latter. As a result, the parastyle is twice as large as the paracone in occlusal view. The metacone is trailed by a distinct cuspule and surrounded buccally by a cingulum, which is not nearly as prominent as that around the paracone. The paracone is also displaced lingually relative to the metacone. The protocone is largely formed by a crest oriented mesiobuccally-distolingually. Its apex tends to be located more towards the distal segment, where the

**Table 3.** Dental measurements, upper teeth (in mm). Measurements for *Siamogale thailandica* were taken from Grohé *et al.* (2010).

Measurements	<i>Siamogale melilutra</i>					<i>Siamogale thailandica</i>	
	ZT-10-03-064b		ZT-09-03-032		IVPP V 23272	Range	Mean
	Left	Right	Left	Right	Right		
I1 mesiodistal length			5.09	5.22			
I1 mediolateral width			4.13	3.98			
I2 mesiodistal length			5.82	6.02			
I2 mediolateral width			4.68	4.50			
I3 mesiodistal length			8.19	8.31			
I3 mediolateral width			5.79	6.12			
P2 maximum mesiodistal length		10.7	10.02			5.2	5.2
P2 maximum mediolateral width		6.6	5.40			2.9	2.9
P3 maximum mesiodistal length	12.0	11.8	11.57	11.94		7.0	7.0
P3 maximum mediolateral width	8.1	7.6	7.51	8.07		4.1	4.1
P4 maximum mesiodistal length	16.0	15.7		14.81		11.1–13.5	12.08
P4 maximum mediolateral width	15.0	15.0		14.43		8.5–11.1	9.68
M1 labial mesiodistal length	14.6	14.2	13.19	13.18	13.65	8.5–12.0	9.73
M1 lingual mesiodistal length	15.8	16.0	14.87	14.97	15.68	10.9–15.9	13.26
M1 maximum mediolateral width	17.4	17.6	17.37	17.47	17.2	12.3–17.8	14.53

preprotocrista and postprotocrista slightly diverge in orientation. There may be a shallow notch at or just mesial of the protocone. The preprotocrista extends mesiobuccally and merges with the mesial cingulum. The postprotocrista, on the other hand, pinches off shortly distal to the protocone apex and completely disappears before reaching the transverse level of the metacone. On the buccal face of the protocone, there is another small ridge leading towards the paracone. There is no discrete hypcone but in its place is a greatly expanded talon that expands distally beyond the metacone, presumably in occlusion with the m2. A distinct lingual cingulum is present, beginning at the mesiolingual corner of the tooth at the base of the preprotocrista and extending lingually then distally to merge with the small cuspule distal to the metacone. This cingulum is particularly thick, although not quite as thick as the buccal cingulum. It is undulating and elevated opposite to the paracone, and occludes with the m1 talonid and m2 trigonid. The lingual and buccal cingula are also decorated by a series of small crenulations, especially along their inner margins (particularly visible on ZT-10-03-064b). The large talon and the broad valley between the postprotocrista and metacone are mostly smooth with only vague crenulations.

**Lower teeth (Table 4; Fig. 10).** IVPP V 23271 affords the best view of the lower teeth, supplemented by a single p4 on IVPP V 23270. The lower teeth of these specimens are nearly unworn, except for the tips of m1 cusps. Only the alveoli of the i1–3 are preserved and they increase in size mesiodistally from i1 to i3, although this size increase

is modest. The alveoli are imbricated, with that of the i2 being shifted lingually. The lower canine is strong and distally recurved, with an oval cross section. There is no ridge on the tooth and fine crenulations are visible on surfaces around the entire tooth.

There are four alveoli anterior to the p4. The two more posterior alveoli are obviously for the p3, whereas the more anterior two represent either a double-rooted p2 or single-rooted p2 and p1. We interpret the two anterior-most alveoli as belonging to a double-rooted p2 because of the thinning septum between the two alveoli and the presence of a faint ridge on the anterior side of the more posterior alveolus, a characteristic of double-rooted cheek teeth, which corresponds to a thin groove on the mesial face of the distal root. If our interpretation is correct, the p1 is lost. The p2–3 roots also display modest imbrication and their long axes are oriented mesiobuccally-distolingually, which may result from the need to accommodate these teeth in a short jaw. The p4 is robust with a single cusp and weak mesial and distal ridges along the length of the cusp. The cusp is much taller than cusps on the m1. There is a weak mesial cingulum and a strong distal cingulum, but the cingula do not encircle the entire tooth.

The m1 is the largest tooth in the jaw, largely as a consequence of its broad proportions due to the widening of the talonid. The trigonid is about half the length of the tooth. The paraconid, protoconid and metaconid on the low-crowned trigonid are about equal in size and height. The carnassial blade is short, showing little shearing function. The paraconid has a rounded base and is cuspidate rather than blade-like. The protoconid has a mesial ridge

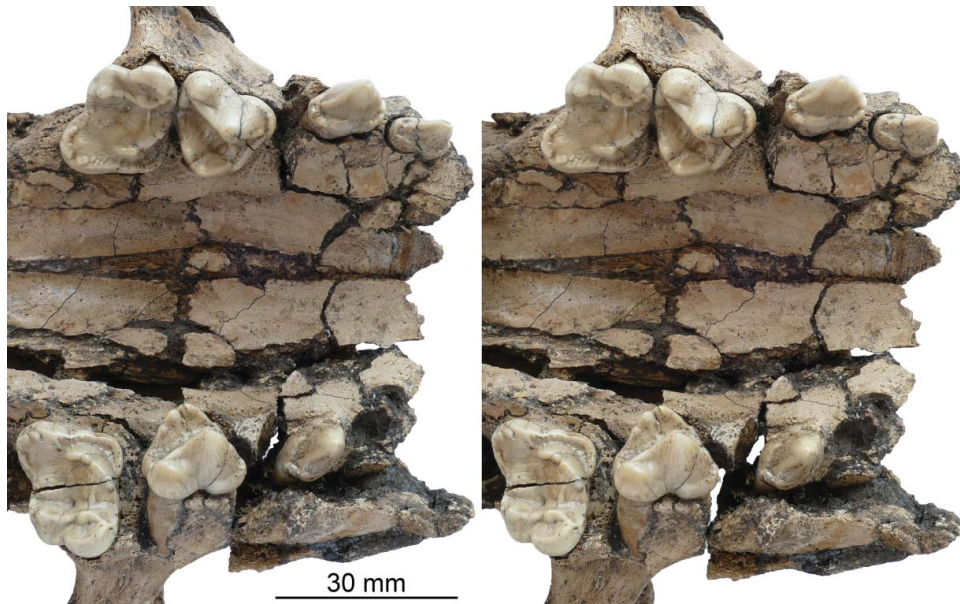


**Figure 8.** Occlusal view of the upper teeth (in stereo view) of *Siamogale melilutra* sp. nov., ZT-10-03-064b, holotype from Shuitangba.

connecting to the paraconid. It also has a lingual ridge reaching to the metaconid. A prominent distal ridge on the protoconid extends distally towards the hypoconid. The metaconid also has a rounded base which is adjacent to that of the paraconid, creating a closed appearance

of the trigonid. The most prominent feature of the m1 is a very strong distal crest emanating from the metaconid that runs distally towards the entoconid crest. This metaconid crest is thickened to form a metastylid at the distolingual aspect of the cusp. A distinct cingulum surrounds much of



**Figure 9.** Occlusal view of the upper teeth (in stereo view) of *Siamogale melilutra* sp. nov., ZT-09-03-032, a referred specimen from Shuitangba. Individual teeth were mounted on light-coloured clay.



**Table 4.** Dental measurements, lower teeth (in mm). Measurements for *Siamogale thailandica* were taken from Grohé *et al.* (2010) and those for the Yushe mandible (THP 19898) were taken from a cast, FM 143941. Alveolar measurements (\*) for *Siamogale melilutra* sp. nov. are not strictly comparable to those of *S. thailandica*.

Measurements	<i>Siamogale melilutra</i>				<i>Siamogale thailandica</i>	
	IVPP V 23271	IVPP V 23270	ZT-07-02-274	THP 19898	Range	Mean
i1 mesiodistal length	2.40*					
i1 mediolateral width	2.03*					
i2 mesiodistal length	4.68*					
i2 mediolateral width	3.23*					
i3 mesiodistal length	4.41*					
i3 mediolateral width	3.73*					
c1 maximum mesiodistal length at base of crown	16.85				7.2	7.2
c1 maximum mediolateral width at base of crown	11.16				5.3	5.3
c1 maximum height from base of crown	25.19					
p2 maximum mesiodistal length	8.84*			9.1	6.8	6.8
p2 maximum mediolateral width	3.90*			5.2	3.9	3.9
p3 maximum mesiodistal length	10.00*			10.1	6.5–8.2	7.48
p3 maximum mediolateral width	5.05*			6.0	3.7–5.0	4.40
p4 maximum mesiodistal length	13.93	14.03		12.7	8.4–10.6	9.44
p4 maximum mediolateral width	7.90	8.45		6.9	4.4–6.7	5.42
m1 maximum mesiodistal length	19.56			19.6	13.9–18.0	16.04
m1 trigonid mesiodistal length	13.00			14.4	8.7–12.2	10.84
m1 maximum mediolateral width	11.90			11.3	7.3–9.8	8.51
m2 maximum mesiodistal length			9.61	9.0*	6.9–11.1	8.50
m2 maximum mediolateral width			9.05	7.1*	6.8–9.6	8.30

the trigonid, except around the metaconid, and there are weak crenulations along much of the cingulum. On the broadened talonid, a relatively small and low-crowned hypoconid is located at the buccal margin, just distal to the postprotocristid. There is a deep notch separating the postprotocristid and the hypoconid. There is no distinct entoconid cusp, which is instead a shallow crest running along the lingual border and extending to the distal border of the talonid. Between the hypoconid and entoconid crest is a broad, smooth basin lacking crenulations. An indistinct cingulum surrounds the hypoconid. A single, large, rounded m2 alveolus indicates a rounded m2, although a thin partial septum on the buccal side reveals the coalescence of two roots. An isolated m2 (ZT-07-02-274) has a single coalesced root with a thin lateral groove, consistent with the m2 alveolar morphology of IVPP V 23271. Based on the presence of this groove, we consider this to be a right m2. The m2 has a rounded, button-shaped and rather flat crown. A slightly elevated rim surrounds the entire tooth with a depression in the middle. If we have oriented this tooth correctly, muted protoconid and hypoconid cusps can be identified along the buccal margin.

**Remarks.** The lack of a carnassial notch on the P4 and loss of M2 place the Shuitangba form in the family Mustelidae. Within the Mustelidae, however, its dental characteristics present a mosaic of features that are unknown among existing clades, except in *Siamogale*. Whereas the P4 morphology invokes that of lutrines, despite a few peculiar details, the M1 recalls those of Old World badgers (melines), particularly the expanded talon distal to the protocone. On the other hand, the new Shuitangba form does not easily fit in known meline clades either; that is, it lacks typical meline dental characters such as a discrete and conical P4 protocone (or, in the case of *Meles*, a very reduced P4 protocone), and the absence of a distally extended M1 postprotocrista (e.g. Wallace & Wang 2004). Cranial characteristics also do not lead to an unambiguous assignment. Whereas a short rostrum and large infraorbital canal are frequently seen in otters, the lack of a sharply narrowed postorbital region of the neurocranium, a feature typical of all known lutrines although it may express differently in different taxa, seemingly casts doubts again about its membership in lutrines.

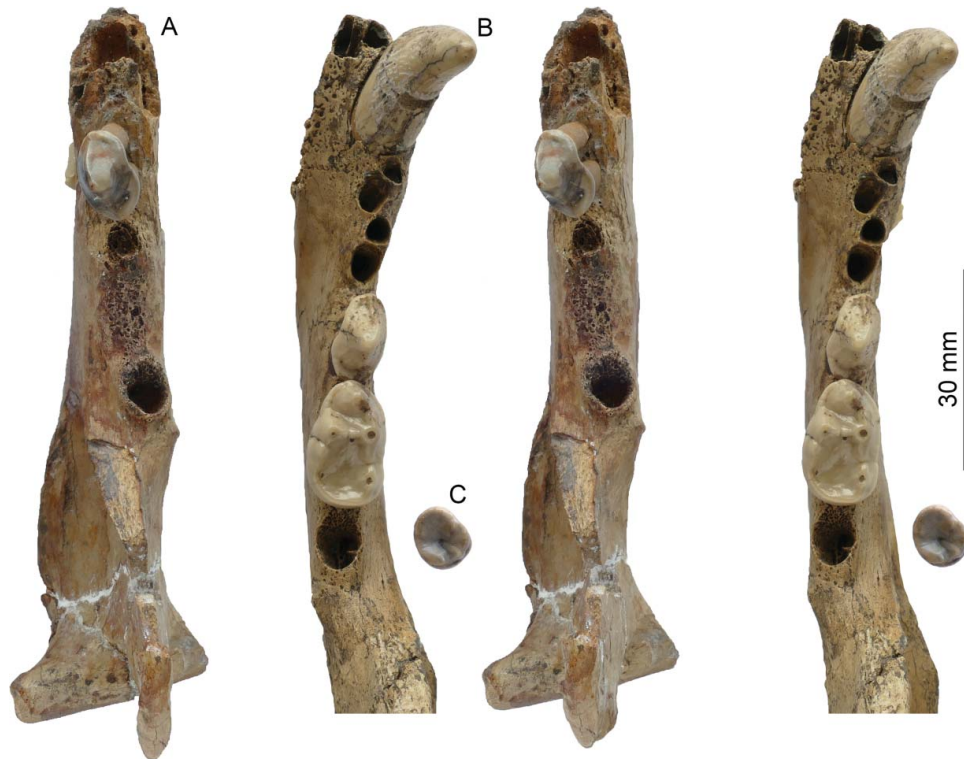


**Figure 10.** Occlusal view of the lower teeth (in stereo view) of *Siamogale melilutra* sp. nov. **A**, IVPP V 23270; **B**, IVPP V 23271; **C**, ZT-07-02-274 (isolated m2); referred specimens from Shuitangba.

However, on balance, lutrine affinity is suggested by the following combination of characters: an enlarged infraorbital canal, ventral extension of the mastoid process beyond the level of the auditory meatus, the mastoid process separated by a broad shelf from the paroccipital process, an anterior position ofinion relative to the lambdoid crest, a straight zygomatic arch (although not all lutrines exhibit this character), robust and short premolars with strong cingula, a short P4 with a large protocone-hypocone crest along the entire lingual border, an enlarged, rectangular M1 with a distally expanded talon and lacking a postprotocrista, and a shortened and broadened m1 talonid. However, numerous detailed differences exist that make referral of *Siamogale* to known lutrine clades problematic. The thick-based P4 protocone crest is quite different from the low, shelf-like crests seen in extant lutrines, except the sea otter *Enhydra lutris*. On the other hand, the upper carnassial is fundamentally different from the highly bunodont carnassials of modern sea otters and fossil Enhyriodontini (Morales & Pickford 2005) from South Asia, Europe and Africa, all of the latter having been previously considered closely related to the extant sea otter. Similarly, with respect to the M1, the massive parastyle, the orientation of the preprotocrista, the medial thickening of lingual cingulum, and the exaggerated expansion of the talon all contribute to a very different configuration from the M1s in living otters and fossil

enhyriodontines. Based on the above, *Siamogale* probably represents a previously unrecognized clade of mustelids that combines cranial and dental features of both lutrines and melines.

Old World Mio–Pleistocene lutrines and other otter-like forms in Asia that warrant close examination include: *Vishnuonyx* from the middle Miocene of the Indian Subcontinent and Thailand, and middle to late Miocene of Kenya; *Sivaonyx* from the middle Miocene of Thailand, the late Miocene of Yunnan, the Indian Subcontinent and Europe, and the late Miocene to early Pleistocene of Africa; *Enhyriodon* from the Plio–Pleistocene of the Indian Subcontinent and probably Africa; ‘*Lutra*’ *aonychoides* from the late Miocene of China; and *Siamogale thailandica* from the late middle Miocene of Thailand (Ginsburg *et al.* 1983; Qi 1983, 1985, 2006; Pickford 2007; Grohé 2011; Grohé *et al.* 2010, 2013). Of these, *Vishnuonyx*, *Sivaonyx* and *Enhyriodon* belong to a clade of their own, the Enhyriodontini of Pickford *et al.* (2007). Morales & Pickford (2005) also include *Paludolutra* in the Enhyriodontini, a taxon that we discuss later in this comparison. *Siamogale* is easily distinguishable from the enhyriodontines (except *Paludolutra*) in its lack of highly cuspidate (conical) P4 protocones and hypocones, a poorly developed P4 parastyle, presence on the M1 of a distally expanded talon and a cusplule that is distal rather than lingual to the metacone, crenulated enamel, lack of a distinct p4 distal accessory

cusps, and the presence of a distal ridge of the metaconid that is continuous with the entoconid crest.

Based on the anterior portions of a partial cranium from the late Miocene locality 49 (PMU 22, Yangmukou, Jijia-gou) of the Baode Basin, Zdansky (1924) named the species '*Lutra*' *aonychoides*. This species does not belong to *Lutra*, as indicated by its strong, discrete P4 protocone, but it has somewhat wrinkled enamel surfaces, as in *Siamogale*. *Siamogale* is notably different from the Baode species in lacking a discrete P4 protocone, which is more mesially located and followed distally by a broadened internal cingulum in '*Lutra*' *aonychoides*. *Siamogale* also exhibits a cuspsule distal to the metacone and thickening of the lingual cingulum on M1, conditions absent in '*Lutra*' *aonychoides*.

Southeast Asia became germane to this matter with the discovery of dental remains of *Siamogale thailandica* from the middle Miocene lignites of Mae Moh in northern Thailand (Ginsburg *et al.* 1983; Ginsburg 1984). Initially described as a lutrine based on a single left m1 (Ginsburg *et al.* 1983), *Siamogale* was later suggested to resemble some European fossil badgers (*Lartetictis* and *Adroverictis*), and the North American *Mionictis* because of their common possession of a basined m1 talonid with a distal ridge on the metaconid that connects with the entoconid crest (Ginsburg & Morales 1996). However, Ginsburg & Morales (1996) placed *Lartetictis* within the Melinae and did not include *Siamogale* in their phylogeny. Pickford (2007, fig. 23), on the other hand, placed *Siamogale* at the base of his Lutrini group (i.e. modern *Lutra*, *Lontra*, *Lutrogale*, *Pteronura* and fossil relatives), but also envisioned an earlier connection of *Siamogale* with his Aonychini group (i.e. modern *Aonyx* and fossil relatives). More recently, Grohé *et al.* (2010) described additional dental materials, including upper cheek teeth, of *Siamogale thailandica* from the type locality. However, despite this increased knowledge, almost 30 years after its initial description, Grohé *et al.* (2010) were still hesitant to place *Siamogale* in a particular clade (Lutrinae, Melinae or Galictinae), settling instead for an ambiguous characterization of 'bunodont otter-like mustelid', and considered it to be closely related to *Mionictis* and *Lartetictis* (see additional comments under Remarks above).

Overall, our new Shuitangba form most closely resembles *Siamogale thailandica* (Ginsburg *et al.* 1983; Grohé *et al.* 2010). Strikingly, the P4s of *S. melilutra* and *S. thailandica* share a protocone crest, and the M1s share a medially thickened and distinctly distally enlarged lingual cingulum, which forms an expanded talon, and the presence of a cuspsule just distal to the metacone. The mandible and lower teeth are similarly striking in their detailed resemblances: an enlarged muscle scar from the superficial masseter and a broadened m1 talonid with a distinct crest emanating distally from the metaconid and connecting to the entoconid crest.

Despite the detailed similarities between the forms from Shuitangba and the Mae Moh Basin, there are also many differences between these two species. The ascending ramus in *Siamogale thailandica* is more vertical in comparison to the more posteriorly inclined condition in *S. melilutra*. The most prominent dental difference is the configuration of the P4 protocone. In *S. thailandica* the P4 has a more or less cuspidate protocone with a broad crest emanating from it distally that ends at the level of the carnassial blade (Grohé *et al.* 2010, fig. 2h1–2). This is in contrast to the condition seen in *S. melilutra*, which does not have as great a distinction between the mesial and distal segments of the protocone crest. Besides the significant size difference between *S. melilutra* and *S. thailandica* (Tables 3, 4), other differences are also easily observable – a broader M1 lingual cingulum in *S. thailandica*, a relatively shortened m1 in *S. melilutra* (Table 4), and an m1 metaconid distal ridge that is subdivided into a discrete cusp (metastylid) in *S. melilutra*.

Other bunodont otters from the Mio–Pliocene of Europe and North America merit comparison with *Siamogale*. From the late Miocene (MN 12) Baccinello V1 faunal assemblage of the Grosseto lignites in Tuscany, Italy, Hürzeler (1987) erected two genera, *Paludolutra* and *Tyrrhenolutra*. The lower carnassials of *Tyrrhenolutra* (Hürzeler 1987, fig. 5) possess a distinct distal ridge along the length of the metaconid, as in *Siamogale*. Moreover, Villalta & Crusafont (1945) described a mandible of *Paludolutra lluecai* from Los Algezares, Teruel, Spain, whose m1 displays both a metaconid distal ridge connected to the entoconid crest and a metastylid, as in *S. melilutra* (refigured in Morales & Pickford 2005, fig. 5; Repenning 1976, fig. 2). The enamel of *Paludolutra* and *Tyrrhenolutra* is crenulated (Hürzeler 1987, fig. 4), especially on the M1, recalling the condition in *Siamogale*. However, both *Paludolutra* and *Tyrrhenolutra* have a less developed M1 lingual cingulum than *Siamogale*, and the M1 cuspsule is lingual rather than distal in *Paludolutra* and absent in *Tyrrhenolutra*. P4 morphology also differs from the crest-like protocone in *Siamogale*. In *Paludolutra* the P4 has a prominent protocone, directly lingual to the latter, and bears a hypocone that is often divided into cuspsules placed lingually to the paracone, while in *Tyrrhenolutra* the protocone and hypocone are closer to each other and positioned lingual to the paracone. Notably, the mesial position of the P4 protocone in *Paludolutra* is also seen in *Paralutra garganensis* from the late Miocene 'Terre Rosse' faunal complex of Gargano, Italy (Willemsen 1983, pl. 1, fig. 3; Villier *et al.* 2011, fig. 2), which may suggest a close relationship between these taxa. *S. melilutra* also shows similarities to *Enhydritherium* from the early Pliocene of North America (Berta & Morgan 1985; Lambert 1997), as *Enhydritherium* also possesses an m1 metaconid distal ridge connected to the entoconid crest, a metastylid on m1 and crenulated enamel. However,

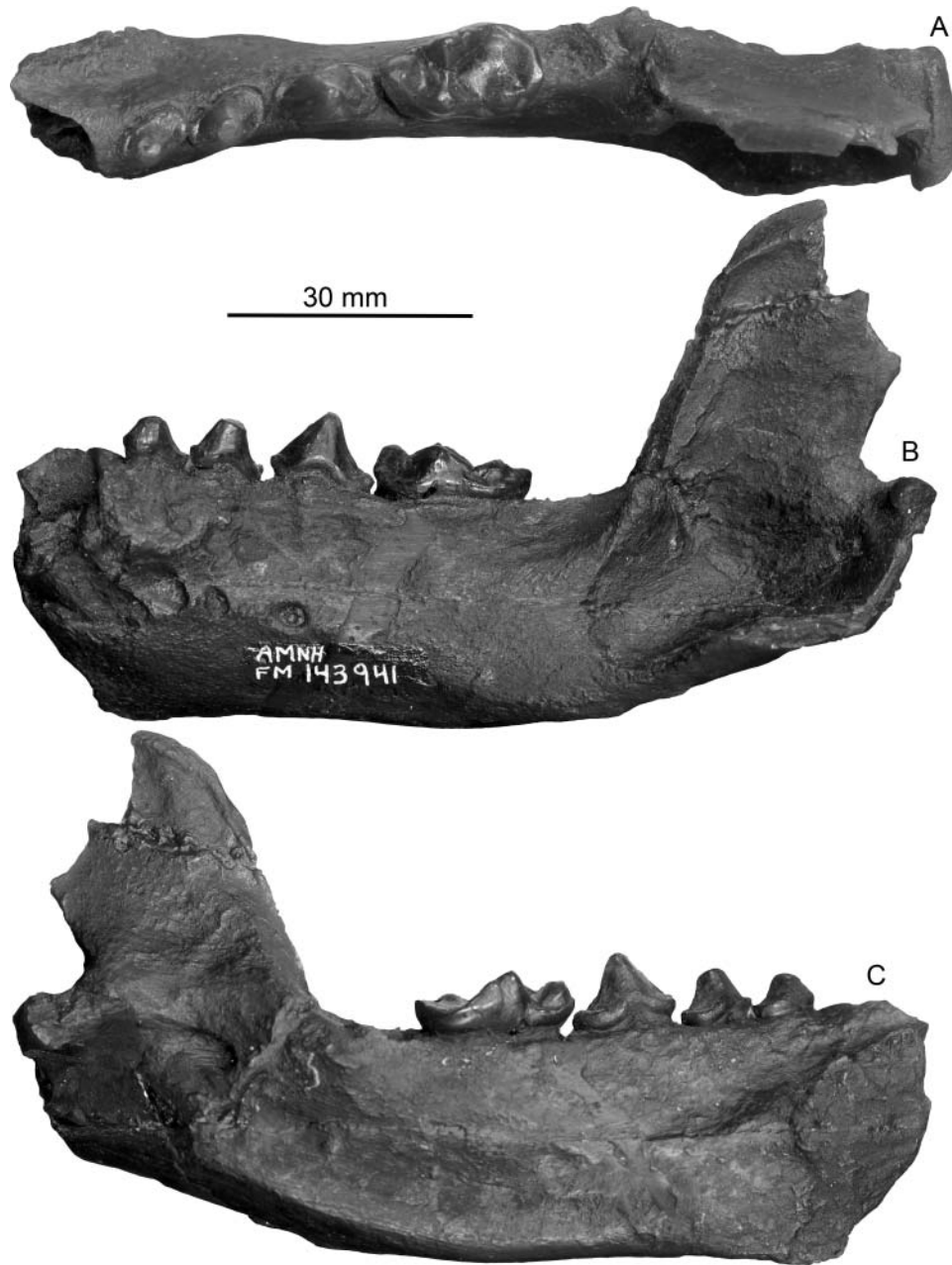


**Figure 11.** *Siamogale melilutra* sp. nov., THP 19898 (AMNH FM cast 143941) from the Yushe Basin. **A**, occlusal, **B**, lateral, and **C**, medial views. Photographs of a polyester cast.

*Enhydritherium* differs from *Siamogale* by the presence of a discrete protocone and hypocone on the P4, a less developed lingual cingulum on M1, and an M1 cusplule in lingual position rather than distal to the metacone.

Finally, Teilhard de Chardin & Leroy (1945) referred a left mandible (THP 19898, Dapinggou, likely from the Pliocene Gaozhuang Formation) (Fig. 11) from the Yushe Basin to '*Lutra*' *aonychoides* Zdansky, apparently based on size (although no comparable lower teeth from Baode or upper teeth from Yushe are known) and what

was perceived at that time as age equivalence (the Yushe specimen is now known to be significantly younger than locality 49 from Baode). Surprisingly, the Yushe specimen matches well with *Siamogale melilutra* down to all cusp details as well as dental dimensions (Table 4). The only appreciable differences are the somewhat smaller p4 with less well-developed cingulum in the Yushe individual and the higher metaconid relative to the protoconid, which are likely due to geographical or temporal variation.

## Phylogeny

In an early attempt at reconstructing higher level relationships of lutrines, de Muizon (1982) envisioned otters as a paraphyletic grouping, but he included then-known ‘musteloid’ taxa, such as phocids and mephitids, that are now known to belong to clades that have no close relationships to otters. A morphological phylogeny of living mustelids by Bryant *et al.* (1993) placed Lutrinae at the terminal end of Mustelidae and as the sister clade to the Melinae (i.e. Old World badgers *Meles* and *Arctonyx*). Most recent molecular phylogenies of mustelids also place the lutrines near the terminal end of the mustelid tree, but as the sister clade of the genus *Mustela* (Koepfli & Wayne 1998; Sato *et al.* 2003, 2009; J. J. Flynn *et al.* 2005; Koepfli *et al.* 2008a), as the sister clade of Ictonychinae (Dragoo & Honeycutt 1997; Koepfli & Wayne 2003; Wolsan & Sato 2010; Sato *et al.* 2012), or as both (Koepfli *et al.* 2008b). If the molecular relationship is correct, then the dental

similarities between badgers and otters must be the result of convergences.

Relationships among the 13 currently recognized extant species of lutrines (Wozencraft 2005) are also not clear. An early attempt using numerical taxonomy (van Zyll de Jong 1987, 1991) differs substantially from that based on the morphology of fossil and extant taxa (Willemsen 1992). Despite the generally unresolved nature of the phylogeny of the latter, Willemsen proposed both a close relationship of *Mionictis* and *Siamogale*, following Ginsburg *et al.* (1983), and that certain fossil and living forms, such as *Paralutra*, *Lutravus*, *Satherium*, *Lutra* and others, are also derived from *Mionictis*. In addition, Willemsen placed the sea otter, *Enhydra*, within the bunodont fossil otter *Vishnuonyx–Enhydriodon–Sivaonyx* clade, as did Berta & Morgan (1985), who also consider a closer relationship between *Enhydritherium* and *Enhydra*. On the other hand, Pickford (2007) proposed that *Vishnuonyx–Sivaonyx–Enhydriodon* are closely related to *Paludolutra* and potentially to *Enhydritherium* and/or *Enhydra*.



**Figure 12.** Artist’s reconstruction of two individuals of *Siamogale melilutra* sp. nov., one of them feeding on a freshwater clam. The tapir in the background is *Tapirus yunnanensis* (Ji *et al.* 2015). Aquatic plants include water chestnut (*Typha*) and fox nut (*Euryale*) (Huang *et al.* 2015), and the low shrub in foreground is Sichuan peppercorn (*Zanthoxylum*). Art by Mauricio Antón.

However, an early mtDNA approach by Koepfli & Wayne (1998), later superseded by a more comprehensive analysis with a wider sampling of genes and taxa (Koepfli *et al.* 2008a, b), embedded the sea otters within the rest of the living otter clade with the striking implication that the bunodont teeth in sea otters were derived from a dental plan not unlike that of most of the living otters, in contradiction to the independent origins of bunodont otters as proposed by Willemsen (1992, fig. 22). Additionally, Pickford (2007) considered *Paralutra* and *Siamogale* to belong to Lutrini (i.e. modern *Lutra*, *Lutrogale*, *Lontra*, *Pteronura* and fossil relatives).

Despite the above efforts, a cladistic framework based on an explicit character matrix of fossil and living otters is still lacking, and our matrix presented here, at the generic and species levels, must necessarily be considered a tentative first attempt because of the still-fragmentary nature of many fossil taxa (see Material and methods). In the parsimony analysis, we found 22 trees with 1638 steps, consistency index (CI) = 0.78 and retention index (RI) = 0.51. The monophyly of Lutrinae (clade 1, Fig. 13A, B) is well supported in the majority consensus tree of the parsimony analysis with a bootstrap value of 88%. Synapomorphies of otters include a large infraorbital canal (character 4, state 1), the dorsal root of the anterior end of zygomatic arch located anterior to the ventral root (character 9, state 1, reversed state in *Siamogale*), inion positioned anteriorly relative to the lambdoid crest (character 11, state 1), the mastoid process expanded ventrally below the auditory meatus (character 14, state 1), a short P4 metastylar blade (character 20, state 1), a distally expanded P4 lingual shelf (character 24, state 1, reversed state in *Paralutra jaegeri* and *Vishnuonyx*), a widened m1 talonid (character 35, state 1), and a deep talonid notch on m1 (character 36, state 1).

*Pteronura brasiliensis* is the most basal extant otter (Fig. 13A, B). It is closely related to *Lontra* species, which are themselves closely related to the clade comprising *Lutra lutra* and *Aonyx capensis* (Fig. 13A). Finally, *Enhydra* is the most derived extant otter. The topology of the Bayesian tree incorporating both extant and fossil taxa shows broadly unresolved relationships among extant otter species. However, a Bayesian analysis performed with extant species only produced the same topology as described for the majority consensus tree. These results are partly consistent with those of Koepfli *et al.* (2008a), the difference being the recovery of *Enhydra* as more basal than *Lutra* and *Aonyx*. Koepfli *et al.* (2008a) used the same set of gene sequences, but in a broader sample of extant mustelids.

Our new fossil species, *Siamogale melilutra*, is closely related to *S. thailandica*, with which it shares a shelf-like P4 protocone (character 22, state 1, convergent with extant otters except *Enhydra lutris*), a cuspule distal to the metacone on M1 (character 31, state 1), and a distal ridge

of the m1 metaconid (character 33, state 1, convergent with *Tyrrhenolutra*, *Paludolutra* and *Enhydritherium*). This relationship is strongly supported (clade 4, Fig. 13A and clade 3, Fig. 13B; bootstrap = 78% for the parsimony analysis; posterior probability = 0.92 for the Bayesian analysis). Additionally, as a result of the parsimony analysis, the European *Paralutra jaegeri* is basal to these eastern Asian otters (clade 3, Fig. 13A). Synapomorphies for clade 3 include the presence of a mesiodistal M1 cingulum (character 28, state 1) and a distally expanded M1 talon (character 29, state 2).

Clade 6 of Figure 13A regrouping *Vishnuonyx*–*Sivaonyx*–*Enhydriondon*–*Enhydra* is supported by the absence of crenulation on M1 (character 30, state 0), the presence of an M1 cuspule lingual to the metacone (character 31, state 2, convergent with *Enhydritherium*–*Paludolutra*), and a distinct p4 distal accessory cusp (character 32, state 1, convergent with *Lontra* and *Enhydra*, and within *Aonyx* individuals). *Enhydriondon* and *Enhydra* (clade 7, Fig. 13A) are further distinguished by the presence of a metastylar notch on P4 (character 21, state 1, convergent with *Paralutra jaegeri*). The Bayesian tree displays a clade *Vishnuonyx*–*Sivaonyx*–*Enhydriondon* (clade 4, Fig. 13B) with an unresolved placement of *Enhydra* within fossil and most of extant otters (clade 2, Fig. 13B). In that case, *Enhydriondon* is basal to *Vishnuonyx* and *Sivaonyx*, which is unexpected given the degree of bunodonty and the stratigraphical occurrence of those genera in the Siwaliks of the Indian subcontinent (*Vishnuonyx* ancestral to *Sivaonyx* and *Enhydriondon* in Willemsen 1992; Pickford 2007).

*Paralutra*, like *Vishnuonyx*, is another genus of otter that has been previously hypothesized to have given rise to one of the main otter clades (e.g. Willemsen 1992; Pickford 2007), but species of *Paralutra* do not constitute a monophyletic group: *Paralutra jaegeri* is basal to the eastern Asian *Siamogale* (clade 3, Fig. 13A), whereas ‘*Paralutra*’ *garganensis* is closely related to *Enhydritherium terranova* and *Paludolutra* species (clade 10, Fig. 13A). These later Italian and North American fossil otters display a low-crowned P4 hypocone (character 26, state 1, convergent with *Enhydra*). Furthermore *Enhydritherium* and *Paludolutra* (clade 11, Fig. 13A) share the presence of a cuspule lingual to the metacone on M1 (character 31, state 2). This relationship is supported both in the parsimony and Bayesian analyses (clades 10 and 11, Fig. 13A; clades 7 and 8, Fig. 13B). In both the parsimony and Bayesian analyses, *Tyrrhenolutra helbingi* is basal to ‘*Paralutra*’ *garganensis*, *Paludolutra* and *Enhydritherium* (clade 9, Fig. 13A; clade 6, Fig. 13B). Additionally, in the majority consensus tree of the parsimony analysis, the clade *Tyrrhenolutra*–‘*Paralutra*’ *garganensis*–*Paludolutra*–*Enhydritherium* (clade 9) is more closely related to the clade *Vishnuonyx*–*Sivaonyx*–*Enhydriondon*–*Enhydra* (clade 6) than to *Paralutra jaegeri*–*Siamogale* (clade 3). Clade 5 of Figure 13A

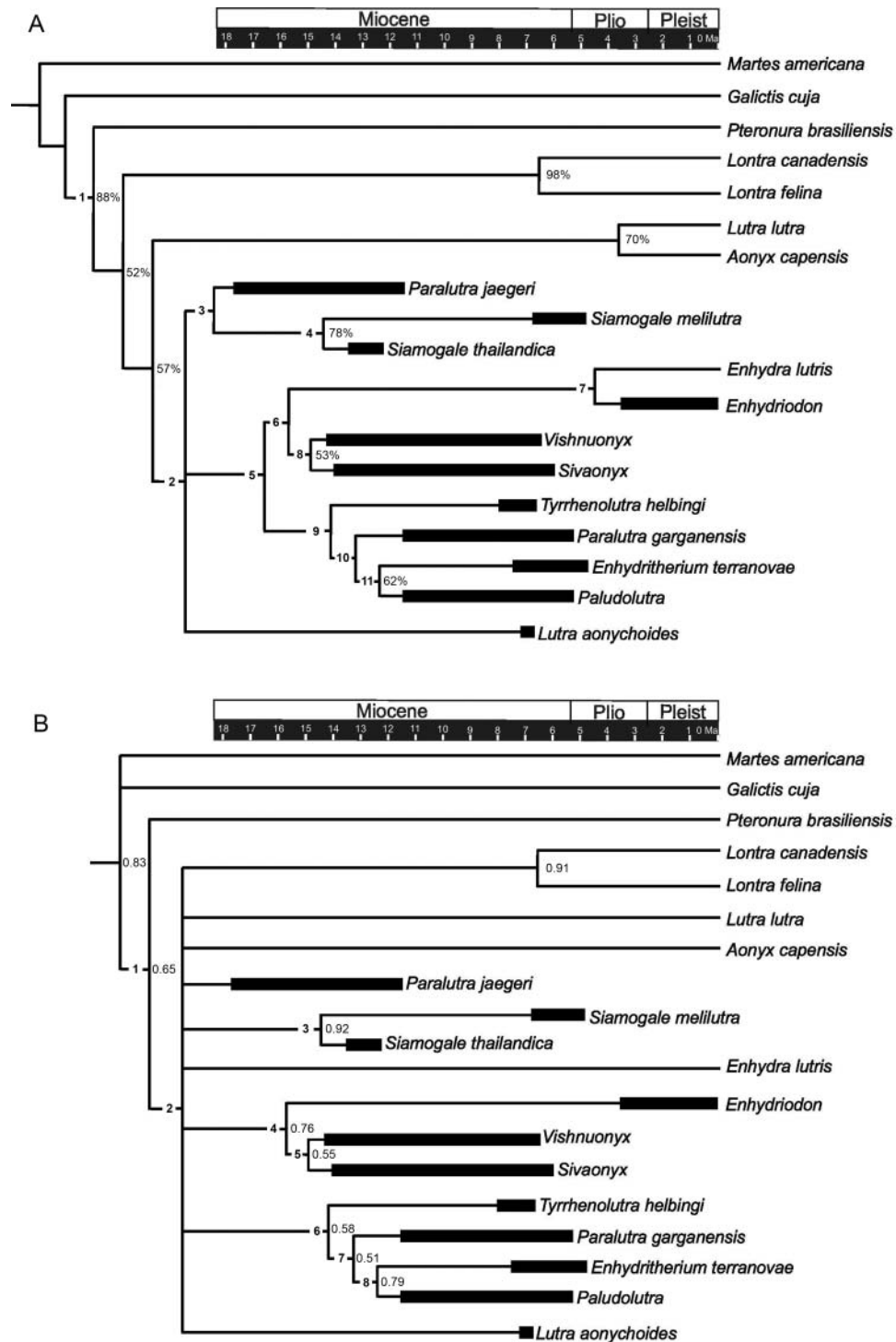


**Figure 13.** Results of the phylogenetic analyses of fossil and extant otters. **A**, 50% majority consensus tree from the 22 most parsimonious trees found by PAUP; bootstrap values of >50% are indicated for nodes. **B**, Bayesian inference phylogeny; posterior probabilities are indicated for each node. Thick black bars indicate the stratigraphical distribution of fossil taxa.

includes otters united by a high-crowned P4 hypocone (character 26, state 2, reversed in '*Paralutra*' *garganensis* and *Enhydra*). Finally, the relationships of *Lutra aonychoides* with our fossil otter sample still remains unresolved (in clade 2 of Fig. 13A, B).

Our phylogeny provides important insights into the evolutionary history of otters. We suggest for the first time that the middle Miocene European species of *Paralutra* are not monophyletic, but rather that '*Paralutra*' *garganensis* represents a basal taxon at the origin of European

and North American fossil otters (*Paludolutra–Enhydritherium*), whereas *Paralutra jaegeri* is in a clade of badger-like eastern Asian fossil otters, including our new species from Yunnan and Yushe. Another major contribution of our phylogenetic analyses concerns the origin of the extant sea otter. *Enhydra* falls into the Eurasian and African fossil clade of *Vishnuonyx–Sivaonyx–Enhydriodon* and, more specifically, is suggested to be closely related to *Enhydriodon*. Our phylogeny is in accordance with those of Willemssen (1992) and Pickford (2007), who proposed a close relationship between *Enhydriodon* and *Enhydra*, but is in contradiction with that of Berta & Morgan (1985), who placed *Enhydriodon* basal to *Enhydritherium* + *Enhydra*. In fact, the lack of a parastyle in *Enhydritherium* and *Enhydra* (character 27 in our matrix – coded as present and large in *Enhydriodon*, contrary to the character state in the phylogeny of Berta & Morgan 1985) is regarded as convergent. Also, *Paludolutra* is usually grouped with *Vishnuonyx–Sivaonyx–Enhydriodon* in the Enhydriodontini (Morales & Pickford 2005), whereas we propose that *Paludolutra* is a sister taxon of *Enhydritherium*. Our phylogeny therefore supports the idea of convergence among bunodont otters from the Miocene to the present. In this scenario, the acquisition of a bunodont dentition occurred at least three times in the evolution of otters: in *Sivaonyx–Enhydriodon–Enhydra*, in *Paludolutra–Enhydritherium*, and in the eastern Asian otter *Siamogale*.

### Chronological, zoogeographical and environmental remarks

The Shuitangba *Siamogale melilutra* is much younger than its Thai sister taxon, *S. thailandica*. The latter is known from the Q–K lignite layers in the Na Khaem Formation (Grohé *et al.* 2010), which fall within a reversed magnetic zone that was correlated to Chron C5AAr (Coster *et al.* 2010) with an Astronomically Tuned Neogene Time Scale (ATNT2012) calibrated age range of 13.36–13.18 Ma (Hilgen *et al.* 2012) in the late middle Miocene. Therefore, *S. melilutra* is likely 6 million years younger than *S. thailandica* and their common ancestor is likely to be much older still.

It is perhaps surprising that the Shuitangba *Siamogale melilutra* has not been recognized from the Lufeng and Yuanmou Miocene hominoid sites in northern Yunnan, but has instead been recorded from the Yushe Basin, 1400 km to the north-east and about 1 million years younger in age (~4.9–5.4 Ma) (Fig. 1). Otters are known from the Shihuiba (Lufeng) site (6.2–6.9 Ma, or 6.25–6.73 Ma in 2012 calibration) (Yue & Zhang 2006; Hilgen *et al.* 2012) and the Yuanmou Basin (7.2–8.2 Ma, or 7.21–8.25 Ma in 2012 calibration) (Yue & Zhang 2006; Hilgen *et al.* 2012), but they are referred to enhydriodontines (Qi 1983, 1985, 2006;

Grohé *et al.* 2013). The linking of the faunas of south-western China to those as far north as the Loess Plateau in Yushe has interesting zoogeographical implications. The Yunnan late Miocene faunas were formerly considered to have substantial Oriental affinities (L. J. Flynn & Wessels 2013) and most faunas from North China differ at high taxonomic levels from their counterparts from the Oriental Province, perhaps due as much to the physical distance as to environmental disparities, with the Yunnan late Neogene assemblages typically representing moist forest environments. Kelley & Gao (2012), however, suggest more complexities in faunal affinities between South China and Southeast Asia, with major differences in the composition of the large-mammal faunas in the two regions during the late Miocene at the level of families and orders. A long-distance dispersal of *Siamogale*, crossing several major East China drainages as well as latitudinal climatic zones, attests to the notable dispersal capability and adaptability of an animal that is not hampered by major geographical features like river systems that may serve as barriers to facultative terrestrial carnivores.

### Acknowledgements

Numerous participants in the field excavations helped in retrieving and preparing the specimens described herein: P.-P. You, Y. Ji, T.-G. Li, Y. Wang, W.-Q. Li, X.-B. Wang and others during the 2007–2010 field seasons; and S.-K. Hou, S.-Q. Wang, Q.-Q. Shi, Z.-H. Li, H.-W. Tong, T.-S. Yu, Lawrence Flynn, W.-Q. Li, Y.-K. Li, L.-Z. Li, S.-K. Chen during the 2015 field season. We thank Y. Ji for preparing and casting the otter specimens. We greatly appreciate the help from Jim Dines of the Natural History Museum of Los Angeles County for access to the modern otter collection in his care and for assistance in securing a loan from the Field Museum of Natural History under the care of William Stanley. We also thank Neil Duncan, Eileen Westwig and Eleanor Hoeger for facilitating access to extant otter specimens from the American Museum of Natural History of New York. Hou Yemao of the IVPP assisted in microCT scanning of two specimens. CG would like to acknowledge Paul M. Velazco, Z. Jack Tseng and J. Angelo Soto-Centeno for advice on phylogeny. The artist's reconstruction was provided by Mauricio Antón, in consultation with Prof. Yong-Jiang Huang for background vegetation. We thank Dorata Dutsch and Kevin Kaiyuan Wang of the University of California at Santa Barbara for help in construction of the Latin name. We gratefully acknowledge Manuel J. Salesa and an anonymous reviewer for comments and suggestions in their careful reviews of this manuscript. Field excavations between 2007 and 2010 were supported by the United States National Science Foundation (BCS 1035897 to DFS and NGJ, BCS 0321893 to F. C. Howell and T.



White, BCS 1227964 to DFS, BCS 1227927 to NGJ., BCS 1227838 to JK), and the Yunnan Natural Science Foundation and Government of Zhaotong (2010CC010 to XJ.). Field excavation in 2015 was supported by special excavation funds from the IVPP, the National Natural Science Foundation of China (41430102), and the governments of Zhaotong and Zhaoyang. Travel and postdoctoral stipends for CG were provided by the National Science Foundation (EAR-0958704) and for XW by the IVPP and the National Science Foundation (EAR-0958704, EAR-1227212).

## Supplemental data

Supplemental material for this article can be accessed at <http://dx.doi.org/10.1080/14772019.2016.1267666>

## References

- Alcalá, L., Montoya, P. & Morales, J. 1994. New large mustelids from the late Miocene of the Teruel Basin (Spain). *Comptes Rendus de l'Académie des Sciences, Paris*, **319**, 1093–1100.
- Baskin, J. A. 1998. Mustelidae. Pp. 152–173 in C. M. Janis, K. M. Scott & L. L. Jacobs (eds) *Evolution of Tertiary mammals of North America, Volume 1: terrestrial carnivores, ungulates, and ungulate like mammals*. Cambridge University Press, Cambridge.
- Berta, A. & Morgan, G. S. 1985. A new sea otter (Carnivora: Mustelidae) from the late Miocene and early Pliocene (Hemphillian) of North America. *Journal of Paleontology*, **59**, 809–819.
- Blainville, H. M. D. D. 1841. *Ostéographie et description iconographique des Mammifère récente et fossiles (Carnivores)*. 2 vols. Arthus Bertrand, Paris, 446 pp. + 15 pls.
- Bonaparte, C. L. J. L. 1838. Synopsis vertebratorum systematis. *Nuovi Annali delle Scienze Naturali, Bologna*, **1**, 105–133.
- Bowdich, T. E. 1821. *An analysis of the natural classifications of Mammalia, for the use of students and travellers*. J. Smith, Paris, 115 pp.
- Bryant, H. N., Russell, A. P. & Fitch, W. D. 1993. Phylogenetic relationships within the extant Mustelidae (Carnivora): appraisal of the cladistic status of the Simpsonian subfamilies. *Zoological Journal of the Linnean Society*, **108**, 301–334.
- Chang, L., Guo, Z., Deng, C., Wu, H., Ji, X., Zhao, Y., Zhang, C., Ge, J., Wu, B., Sun, L. & Zhu, R. 2015. Pollen evidence of the palaeoenvironments of *Lufengpithecus lufengensis* in the Zhaotong Basin, southeastern margin of the Tibetan Plateau. *Palaeogeography, Palaeoclimatology, Palaeoecology*, **435**, 95–104.
- Chow, M.-C. & Zhai, R.-J. 1962. Early Pleistocene mammals of Chaotung, Yunnan, with notes on some Chinese stegodonts. *Vertebrata Palasiatica*, **6**, 138–147.
- Colbert, E. H. & Hooijer, D. A. 1953. Pleistocene mammals from the limestone fissures of Szechwan, China. *Bulletin of the American Museum of Natural History*, **102**, 1–134.
- Cook, H. J. & Macdonald, J. R. 1962. New Carnivora from the Miocene and Pliocene of western Nebraska. *Journal of Paleontology*, **36**, 560–567.
- Coster, P., Benammi, M., Chaimanee, Y., Yamee, C., Chavasseau, O., Emonet, E.-G. & Jaeger, J.-J. 2010. A complete magnetic-polarity stratigraphy of the Miocene continental deposits of Mae Moh Basin, northern Thailand, and a reassessment of the age of hominoid-bearing localities in northern Thailand. *Geological Society of America Bulletin*, **122**, 1180–1191.
- Dai, S. & Chou, C.-L. 2007. Occurrence and origin of minerals in a chamosite-bearing coal of Late Permian age, Zhaotong, Yunnan, China. *American Mineralogist*, **92**, 1253–1261.
- Dong, W., Ji, X.-P., Jablonski, N. G., Su, D. F. & Li, W.-Q. 2014. New materials of the Late Miocene *Muntiacus* from Zhaotong hominoid site in southern China. *Vertebrata Palasiatica*, **52**, 316–327.
- Dragoo, J. W. & Honeycutt, R. L. 1997. Systematics of mustelid-like carnivores. *Journal of Mammalogy*, **78**, 426–443.
- Fahlbusch, V. 1967. Über einen *Potamotherium*-Kiefer (Carnivora, Mamm.) aus dem Obermiocän von Reichenstetten bei Regensburg. *Mitteilungen der Bayerischen Staatssammlung für Paläontologie und Historische Geologie*, **7**, 193–200.
- Falconer, H. 1868. *Palaeontological memoirs and notes of the late Hugh Falconer, with a biographical sketch of the author. Vol. I. Fauna Antiqua Sivalensis*. Robert Hardwicke, London, 675 pp.
- Fischer von Waldheim, G. 1817. *Adversaria zoologica. Mémoires de la Société Imperiale des Naturalistes de Moscou*, **5**, 357–472.
- Flower, W. H. 1869. On the value of the characters of the base of the cranium in the classification of the order Carnivora, and on the systematic position of *Bassaris* and other disputed forms. *Proceedings of the Zoological Society of London*, **1869**, 4–37.
- Flynn, J. J., Finarelli, J. A., Zehr, S., Hsu, J. & Nedbal, M. A. 2005. Molecular phylogeny of the Carnivora (Mammalia): assessing the impact of increased sampling on resolving enigmatic relationships. *Systematic Biology*, **54**, 317–327.
- Flynn, L. J. & Wessels, W. 2013. Chapter 18. Paleobiogeography and South Asian small mammals: Neogene altitudinal faunal variation. Pp. 445–460 in X.-M. Wang, L. J. Flynn & M. Fortelius (eds) *Fossil mammals of Asia: Neogene biostratigraphy and chronology*. Columbia University Press, New York.
- Galtier, N., Gouy, M. & Gautier, C. 1996. SeaView and Phylo\_win, two graphic tools for sequence alignment and molecular phylogeny. *Computer Applications in the Biosciences*, **12**, 543–548.
- Geraads, D., Alemseged, Z., Bobe, R. & Reed, D. 2011. *Enhydriodon dikikae*, sp. nov. (Carnivora: Mammalia), a gigantic otter from the Pliocene of Dikika, lower Awash, Ethiopia. *Journal of Vertebrate Paleontology*, **31**, 447–453.
- Ginsburg, L. 1961. La faune des carnivores Miocènes de Sansan (Gers). *Mémoires du Muséum National d'Histoire Naturelle, Série C, Geologie*, **9**, 1–187.
- Ginsburg, L. 1968. Les mustélidés piscivores du Miocène Français. *Bulletin du Muséum national d'Histoire naturelle, Paris, Series 2*, **40**, 228–238.
- Ginsburg, L. 1984. Les faunes tertiaires du Nord de la Thaïlande. *Mémoires de la Société Géologique de France (Nouvelle Série)*, **147**, 67–69.
- Ginsburg, L. 1999. Order Carnivora. Pp. 109–148 in G. E. Rössner & K. Heissig (eds) *The Miocene land mammals of Europe*. Verlag Dr. Friedrich Pfeil, Munich.
- Ginsburg, L. & Bulot, C. 1982. Les carnivores du miocène de Bézian près de la Romieu (Gers, France). *Proceedings of the Koninklijke Nederlandse Akademie van Wetenschappen B*, **85**, 53–76.

- Ginsburg, L. & Morales, J.** 1992. Contribution à la connaissance des Mustélidés (Carnivora, Mammalia) du Miocène d'Europe *Trochictis* et *Ischyriactis*, genres affines et genres nouveaux. *Comptes Rendus de l'Académie des Sciences*, **315**, 111–116.
- Ginsburg, L. & Morales, J.** 1996. *Lartetictis* et *Adroverictis*, nouveaux genres de Melinae (Mustelidae, Carnivora, Mammalia) du Miocène de l'Ancien Monde. *Bulletin du Muséum national d'Histoire naturelle, Paris, Section C*, **4**, 663–671.
- Ginsburg, L. & Morales, J.** 2000. Origine et évolution des Melinae (Mustelidae, Carnivora, Mammalia). *Comptes Rendus de l'Académie des Sciences II, Sciences de la Terre et des Planètes*, **330**, 221–225.
- Ginsburg, L., Invagat, R. & Tassy, P.** 1983. *Siamogale thailandica*, nouveau Mustelidae (Carnivora, Mammalia) néogène du Sud-Est asiatique. *Bulletin de la Société Géologique de France*, **7**, 953–956.
- Grohé, C.** 2011. *Les Hyaenodontida de l'Eocène Libyen et les Carnivora du Miocène moyen d'Asie du Sud-Est : systématique et implications paléobiogéographiques*. Unpublished PhD thesis, Université Poitiers, 263 pp.
- Grohé, C., Bonis, L. de, Chaimanee, Y., Blondel, C. & Jaeger, J.-J.** 2013. The oldest Asian Sivaonyx (Lutrinae, Mustelidae): a contribution to the evolutionary history of bunodont otters. *Palaeontologia Electronica*, **16**, 29A.
- Grohé, C., Chaimanee, Y., Bonis, L. de, Yamee, C., Blondel, C. & Jaeger, J.-J.** 2010. New data on Mustelidae (Carnivora) from Southeast Asia: *Siamogale thailandica*, a peculiar otter-like mustelid from the late middle Miocene Mae Moh Basin, northern Thailand. *Naturwissenschaften*, **97**, 1003–1015.
- Harrison, J. A.** 1981. A review of the extinct wolverine, *Plesio-gulo* (Carnivora: Mustelidae), from North America. *Smithsonian Contributions to Paleobiology*, **46**, 1–27.
- Heizmann, E. P. J. & Morlo, M.** 1998. Die semiaquatische *Lartetictis dubia* (Mustelinae, Carnivora, Mammalia) vom Goldberg/Ries (Baden-Württemberg). *Mainzer Naturwissenschaftliches Archiv*, **21**, 141–153.
- Helbing, H.** 1936. Die carnivoren des Steinheimer beckens, A. Mustelidae. *Palaeontographica Beiträge zur Naturgeschichte der vorzeit*, **5**, 1–56.
- Hilgen, F. J., Lourens, L. J., Van Dam, J. A., Beu, A. G., Foyes, A. F., Cooper, R. A., Krijgsman, W., Ogg, J. G., Piller, W. E. & Wilson, D. S.** 2012. The Neogene Period. Pp. 923–978 in F. M. Gradstein, J. G. Ogg, M. D. Schmitz & G. M. Ogg (eds) *The geologic time scale 2012, Volume 2*. Elsevier, Amsterdam.
- Holmes, T., Jr.** 1988. *Sexual dimorphism in North American weasels with a phylogeny of the Mustelidae*. Unpublished PhD dissertation, University of Kansas, Lawrence, 323 pp.
- Huang, Y., Ji, X., Su, T., Wang, L., Deng, C., Li, W., Luo, H. & Zhou, Z.** 2015. Fossil seeds of *Euryale* (Nymphaeaceae) indicate a lake or swamp environment in the late Miocene Zhaotong Basin of southwestern China. *Science Bulletin*, **60**, 1768–1777.
- Hunt, R. M., Jr.** 1974. The auditory bulla in Carnivora: an anatomical basis for reappraisal of carnivore evolution. *Journal of Morphology*, **143**, 21–76.
- Hürzeler, J.** 1987. Die Lutrinen (Carnivora, Mammalia) aus dem 'Grosseto-Lignit' der Toscana. *Schweizerische Paläontologische Abhandlungen*, **110**, 29–48.
- Jablonski, N. G., Su, D. F., Flynn, L. J., Ji, X., Deng, C., Kelley, J., Zhang, Y., Yin, J., You, Y. & Yang, X.** 2014. The site of Shuitangba (Yunnan, China) preserves a unique, terminal Miocene fauna. *Journal of Vertebrate Paleontology*, **34**, 1251–1257.
- Ji, X.-P., Jablonski, N. G., Su, D. F., Deng, C.-L., Flynn, L. J., You, Y.-S. & Kelley, J.** 2013. Juvenile hominoid cranium from the terminal Miocene of Yunnan, China. *Chinese Science Bulletin*, **58**, 3771–3779.
- Ji, X.-P., Jablonski, N. G., Tong, H.-W., Su, D. F., Ebbestad, J. O. R., Liu, C.-W. & Yu, T.-S.** 2015. *Tapirus yunnanensis* from Shuitangba, a terminal Miocene hominoid site in Zhaotong, Yunnan Province of China. *Vertebrata Palasiatica*, **53**, 177–192.
- Kelley, J. & Gao, F.** 2012. Juvenile hominoid cranium from the late Miocene of southern China and hominoid diversity in Asia. *Proceedings of the National Academy of Sciences*, **109**, 6882–6885.
- Koepfli, K.-P. & Wayne, R. K.** 1998. Phylogenetic relationships of otters (Carnivora: Mustelidae) based on mitochondrial cytochrome b sequences. *Journal of Zoology*, **246**, 401–416.
- Koepfli, K.-P. & Wayne, R. K.** 2003. Type I Sts markers are more informative than Cytochrome b in phylogenetic reconstruction of the Mustelidae (Mammalia: Carnivora). *Systematic Biology*, **52**, 571–593.
- Koepfli, K.-P., Deere, K. A., Slater, G. J., Begg, C., Begg, K., Grassman, L., Lucherini, M., Veron, G. & Wayne, R. K.** 2008a. Multigene phylogeny of the Mustelidae: Resolving relationships, tempo and biogeographic history of a mammalian adaptive radiation. *BMC Biology*, **6**, 1–22.
- Koepfli, K.-P., Kanchanasaka, B., Sasaki, H., Jacques, H., Louie, K. D. Y., Hoai, T., Dang, N. X., Geffen, E., Gutleb, A., Han, S.-Y., Heggberget, T. M., LaFontaine, L., Lee, H., Melisch, R., Ruiz-Olmo, J., Santos-Reis, M., Sidorovich, V. E., Stubbe, M. & Wayne, R. K.** 2008b. Establishing the foundation for an applied molecular taxonomy of otters in Southeast Asia. *Conservation Genetics*, **9**, 1589–1604.
- Lambert, W. D.** 1997. The osteology and paleoecology of the giant otter *Enhydritherium terraenovae*. *Journal of Vertebrate Paleontology*, **17**, 738–749.
- Lewis, P. O.** 2001. A likelihood approach to estimating phylogeny from discrete morphological character data. *Systematic Biology*, **50**, 913–925.
- Maddison, W. P. & Maddison, D. R.** 2015. *Mesquite: a modular system for evolutionary analysis*. Version 3.02 (build 681) [updated at <http://mesquiteproject.org>, accessed 19 August 2014].
- Matthew, W. D.** 1924. Third contribution to the Snake Creek fauna. *Bulletin of the American Museum of Natural History*, **50**, 59–210.
- Matthew, W. D.** 1929. Critical observations upon Siwalik mammals. *Bulletin of the American Museum of Natural History*, **56**, 437–560.
- Morales, J. & Pickford, M.** 2005. Giant bunodont Lutrinae from the Mio-Pliocene of Kenya and Uganda. *Estudios Geológicos*, **61**, 233–246.
- Muizon, C. de.** 1982. Les relations phylogénétiques des Lutrinae (Mustelidae, Mammalia). *Geobios, Mémoire Spécial*, **6**, 259–277.
- Nylander, J. A. A.** 2008. *MrModeltest v2.3*. Department of Systematic Zoology, EBC, Uppsala University, Sweden. Original code by David Posada, Universidade de Vigo, Spain.
- Opdyke, N. D., Huang, K. & Tedford, R. H.** 2013. Chapter 4. The paleomagnetism and magnetic stratigraphy of the late Cenozoic sediments of the Yushe Basin, Shanxi Province, China. Pp. 69–78 in R. H. Tedford, Z.-X. Qiu & L. J. Flynn (eds) *Late Cenozoic Yushe Basin, Shanxi Province, China*:

- geology and fossil mammals. Volume I: history, geology, and magnetostratigraphy.* Springer, New York.
- Peigné, S., Bonis, L. de, Likius, A., Mackaye, H. T., Vignaud, P. & Brunet, M.** 2008. Late Miocene Carnivora from Chad: Lutrinae (Mustelidae). *Zoological Journal of the Linnean Society*, **152**, 793–846.
- Pickford, M.** 2007. Revision of the Mio–Pliocene bunodont otter-like mammals of the Indian Subcontinent. *Estudios Geológicos*, **63**, 83–127.
- Pilgrim, G. E.** 1932. The fossil Carnivora of India. *Memoirs of the Geological Survey of India, Palaeontologia Indica, New Series*, **18**, 1–232.
- Qi, G.-Q.** 1983. Description of Carnivora fossils from Lufeng. *Acta Anthropologica Sinica*, **2**, 11–20.
- Qi, G.-Q.** 1985. A preliminary report on Carnivora from the *Ramapithecus* locality, Lufeng, Yunnan. *Acta Anthropologica Sinica*, **4**, 33–43.
- Qi, G.-Q.** 2006. Order Carnivora. Pp. 148–177 in G.-q. Qi & W. Dong (eds) *Lufengpithecus huiyuanensis site*. Science Press, Beijing.
- Rambaut, A., Suchard, M. A., Xie, W. & Drummond, A. J.** 2013. *Tracer, MCM Trace Analysis Tool*. Version v. 1.6.0 [updated at <http://tree.bio.ed.ac.uk/software/tracer>, accessed 1 April 2016].
- Repenning, C. A.** 1976. *Enhydra* and *Enhydriodon* from the Pacific coast of North America. *Journal of Research of the United States Geological Survey*, **4**, 305–315.
- Roman, F. & Viret, J.** 1934. La faune des Mammifère du Burdigalien de la Romieu (Gers). *Mémoires de la Société Géologique de France, Nouvelle Série*, **21**, 1–67.
- Ronquist, F., Teslenko, M., van der Mark, P., Ayres, D. L., Darling, A., Höhna, S., Larget, B., Liu, L., Suchard, M. A. & Huelsenbeck, J. P.** 2012. MrBayes 3.2: efficient Bayesian phylogenetic inference and model choice across a large model space. *Systematic Biology*, **61**, 539–542.
- Ryan, W. B. F., Carbotte, S. M., Coplan, J. O., O'Hara, S., Melkonian, A., Arko, R., Weissel, R. A., Ferrini, V., Goodwillie, A., Nitsche, F., Bonczkowski, J. & Zemsky, R.** 2009. Global Multi-resolution topography synthesis. *Geochemistry, Geophysics, Geosystems*, **10**.
- Rybczynski, N., Dawson, M. R. & Tedford, R. H.** 2009. A semi-aquatic Arctic mammalian carnivore from the Miocene epoch and origin of Pinnipedia. *Nature*, **458**, 1021–1024.
- Salesa, M. J., Antón, M., Siliceo, G., Pesquero, M. D., Morales, J. & Alcalá, L.** 2013. A non-aquatic otter (Mammalia, Carnivora, Mustelidae) from the Late Miocene (Vallesian, MN 10) of La Roma 2 (Alfambra, Teruel, Spain): systematics and functional anatomy. *Zoological Journal of the Linnean Society*, **169**, 448–482.
- Sato, J. J., Hosoda, T., Wolsan, M., Tsuchiya, K., Yamamoto, Y. & Suzuki, H.** 2003. Phylogenetic relationships and divergence times among mustelids (Mammalia: Carnivora) based on nucleotide sequences of the nuclear interphotoreceptor retinoid binding protein and mitochondrial cytochrome *b* genes. *Zoological Science*, **20**, 243–264.
- Sato, J. J., Wolsan, M., Minami, S., Hosoda, T., Sinaga, M. H., Hiyama, K., Yamaguchi, Y. & Suzuki, H.** 2009. Deciphering and dating the red panda's ancestry and early adaptive radiation of Musteloidea. *Molecular Phylogenetics and Evolution*, **53**, 907–922.
- Sato, J. J., Wolsan, M., Prevosti, F. J., D'Elia, G., Begg, C., Begg, K., Hosoda, T., Campbell, K. L. & Suzuki, H.** 2012. Evolutionary and biogeographic history of weasel-like carnivores (Musteloidea). *Molecular Phylogenetics and Evolution*, **63**, 745–757.
- Savage, R. J. G.** 1957. The anatomy of *Potamotherium* an Oligocene lutrine. *Proceedings of the Zoological Society of London*, **129**, 151–244.
- Schindelin, J., Arganda-Carreras, I., Frise, E., Kaynig, V., Longair, M., Pietzsch, T., Preibisch, S., Rueden, C., Saalfeld, S., Schmid, B., Tinevez, J. Y., White, D. J., Hartenstein, V., Eliceiri, K., Tomancak, P. & Cardona, A.** 2012. Fiji: an open-source platform for biological-image analysis. *Nat Methods*, **9**, 676–682.
- Shi, M.-Z., Guan, J., Pan, R.-Q. & Tang, D.-Z.** 1981. Pliocene mammals collected from lignite in Zhaotung, Yunnan. *Memoirs of Beijing Natural History Museum*, **11**, 1–15.
- Smith, K., Czaplewski, N. J. & Cifelli, R. L.** 2014. Middle Miocene carnivores from the Monarch Mill Formation, Nevada. *Acta Palaeontologica Polonica*, **61**, 231–252.
- Sokolov, I. I.** 1973. Evolutionary trends and the classification of the subfamily Lutrinae (Mustelidae, Fissipedia). *Biulletin Moskovskoe Obshchestvo Ispytateĭ Prirody, Otdel Biologicheskii*, **78**, 45–52.
- Stach, J.** 1951. *Arctomeles pliocaenicus*, nowy rodzaj i gatunek z podrodziny borsukowatych, Studia nad trzeciorzędowa fauna brekcyj kostnej w wejśscowosci Weze koło Działoszyna Czesc I. *Acta Geologica Polonica*, **2**, 129–157.
- Storz, J. F. & Wozencraft, W. C.** 1999. *Melogale moschata*. *Mammalian Species*, **631**, 1–4.
- Swofford, D. L.** 2002. *PAUP\*: Phylogenetic analysis using parsimony (\*and other methods)*. Version 4.0b10. Sinauer Associates, Sunderland.
- Tedford, R. H.** 1976. Relationship of pinnipeds to other carnivores (Mammalia). *Systematic Zoology*, **25**, 363–374.
- Tedford, R. H. & Harington, C. R.** 2003. An Arctic mammal fauna from the Early Pliocene of North America. *Nature*, **425**, 388–390.
- Teilhard de Chardin, P. & Leroy, P.** 1945. Les Mustélidés de Chine. *Publications de l'Institut de Géobiologie*, **12**, 1–56.
- Thenius, E.** 1949a. Die Carnivoren von Göriach (Steiermark). Beiträge zur Kenntnis der Säugetierreste des steirischen Tertiärs IV. *Sitzungsberichte der Akademie der Wissenschaften mathematisch-naturwissenschaftliche Klasse*, **158**, 695–762.
- Thenius, E.** 1949b. Die Lutrinen des steirischen Tertiärs (Beiträge zur Kenntnis der Säugetierreste des steirischen Tertiärs I.). *Sitzungsberichte der Akademie der Wissenschaften mathematisch-naturwissenschaftliche Klasse*, **158**, 299–322.
- Thomas, H., Sen, S., Khan, M., Battail, B. & Ligabure, G.** 1982. Part III, The lower Miocene fauna of Al-Sarrar (Eastern Province, Saudi Arabia). *Atlat: The Journal of Saudi Arabian Archaeology*, **4**, 109–136.
- Tseng, Z. J., Wang, X. & Stewart, J. D.** 2009. A new immigrant mustelid (Carnivora, Mammalia) from the middle Miocene Temblor Formation of central California. *PaleoBios*, **29**, 13–23.
- van Zyll de Jong, C. G.** 1987. A phylogenetic study of the Lutrinae (Carnivora; Mustelidae) using morphological data. *Canadian Journal of Zoology*, **65**, 2536–2544.
- van Zyll de Jong, C. G.** 1991. A brief review of the systematics and a classification of the Lutrinae. Pp. 79–83 in C. Reuther & R. Röchert (eds) *Proceedings of the V International Otter Colloquium, Habitat 6*. Hankensbüttel 1989.
- Villalta Comella, J. F. D. & Crusafont-Pairó, M.** 1945. *Enhydriodon lluecai* n. sp. el primer lútrido del Pontiense español. *Boletín de la Real Sociedad Española de Historia Natural (Geología)*, **43**, 383–396.
- Villier, B., Pavia, M. & Rook, L.** 2011. New remains of *Paralu-tra garganensis* Willemsen, 1983 (Mustelidae, Lutrinae) from

- the Late Miocene 'Terre Rosse' of Gargano (Apulia, Italy). *Bollettino della Società Paleontologica Italiana*, **50**, 135–143.
- Wallace, S. C. & Wang, X.** 2004. Two new carnivores from an unusual late Tertiary forest biota in eastern North America. *Nature*, **431**, 556–559.
- Wang, S.-Q., Ji, X.-P., Jablonski, N. G., Su, D. F., Ge, J.-Y., Ding, C.-F., Yu, T.-S., Li, W.-Q. & Duangkrayom, J.** 2015. The oldest cranium of *Sinomastodon* (Proboscidea, Gomphotheriidae), discovered in the uppermost Miocene of southwestern China: Implications for the origin and migration of this taxon. *Journal of Mammalian Evolution*, 1–19.
- Willemsen, G. F.** 1983. *Paralutra garganensis* sp. nov. (Mustelidae, Lutrinae): a new otter from the Miocene of Gargano, Italy. *Scripta Geologica*, **72**, 1–8.
- Willemsen, G. F.** 1992. A revision of the Pliocene and Quaternary Lutrinae from Europe. *Scripta Geologica*, **101**, 1–115.
- Wilson, R. L.** 1968. Systematics and faunal analysis of a lower Pliocene vertebrate assemblage from Trego County, Kansas. *University of Michigan Contributions from the Museum of Paleontology*, **22**, 75–126.
- Wolsan, M. & Sato, J. J.** 2010. Effects of data incompleteness on the relative performance of parsimony and Bayesian approaches in a supermatrix phylogenetic reconstruction of Mustelidae and Procyonidae (Carnivora). *Cladistics*, **26**, 168–194.
- Wozencraft, W. C.** 2005. Order Carnivora. Pp. 532–628 in D. E. Wilson & D. M. Reeder (eds) *Mammal species of the world, a taxonomic and geographic reference*. 3rd edition. Johns Hopkins University Press, Baltimore.
- Yue, L.-P. & Zhang, Y.-X.** 2006. Paleomagnetic dating of *Lufengpithecus lufengensis* fossil strata. Pp. 252–255 in G.-Q. Qi & W. Dong (eds) *Lufengpithecus hudienensis site*. Science Press, Beijing.
- Zdansky, O.** 1924. Jungtertiäre carnivoren Chinas. *Palaeontologia Sinica, Series C*, **2**, 1–149.
- Zhang, C., Guo, Z., Deng, C., Ji, X., Wu, H., Paterson, G. A., Chang, L., Li, Q., Wu, B. & Zhu, R.** 2016. Clay mineralogy indicates a mildly warm and humid living environment for the Miocene hominoid from the Zhaotong Basin, Yunnan, China. *Scientific Reports*, **6**, 20012.